

Side-Chain Halogen Effects on Self-Assembly and Hydrogelation of Cationic Phenylalanine Derivatives

Brittany L. Abraham,^a Samantha G. Mensah,^a Benjamin R. Gwinnell,^a and Bradley L. Nilsson^{a,b*}

^aDepartment of Chemistry, University of Rochester, Rochester, NY 14627, USA.

^bMaterials Science Program, University of Rochester, Rochester, NY 14627, USA.

E-mail: bradley.nilsson@rochester.edu

Tel. +1 585 276-3053

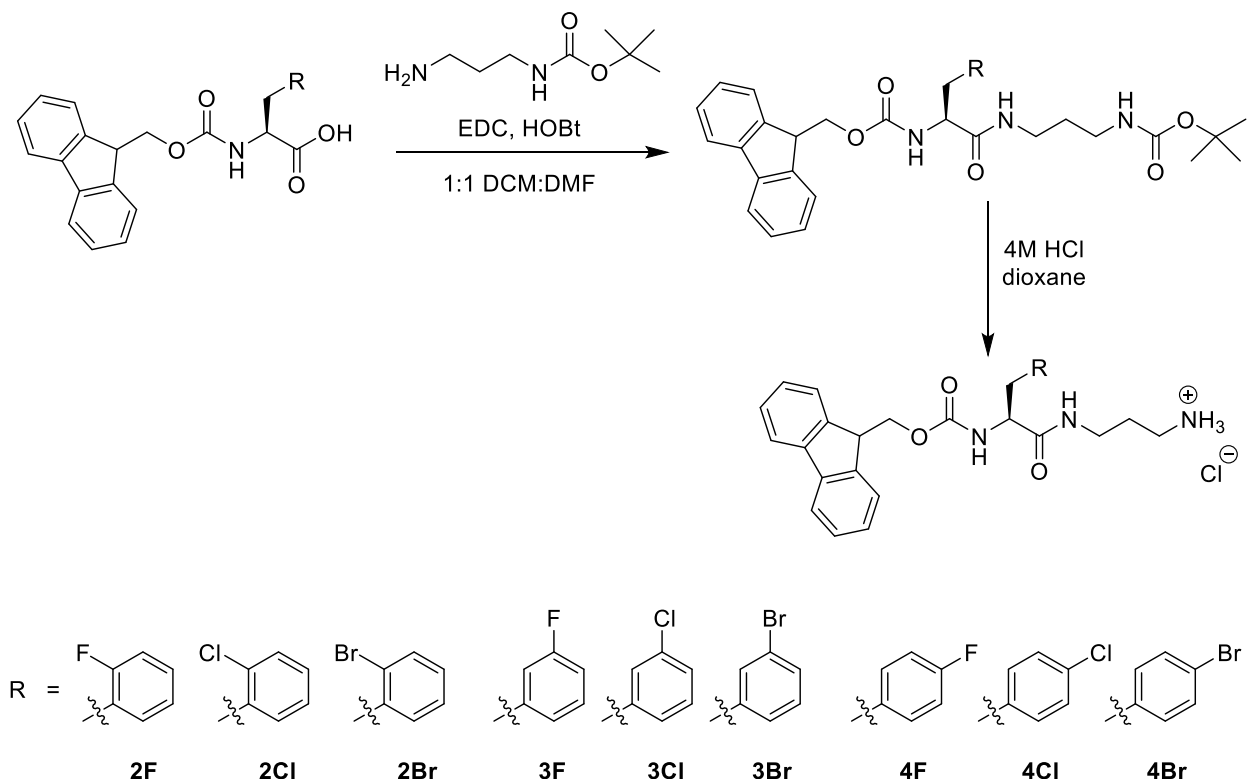
ELECTRONIC SUPPLEMENTARY INFORMATION

Contents:

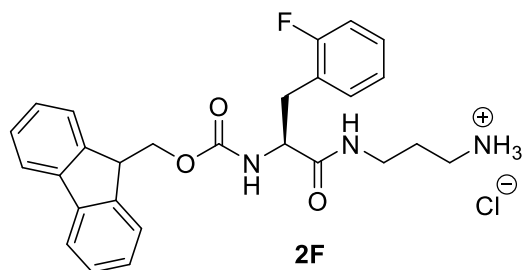
Scheme S1. Synthesis of Fmoc-X-Phe-DAP derivatives 2X–4X	page S3
Figure S1. ¹ H NMR spectrum of Fmoc-2F-Phe-DAP (2F).....	page S8
Figure S2. ¹³ C NMR spectrum of Fmoc-2F-Phe-DAP (2F).....	page S9
Figure S3. ¹⁹ F NMR spectrum of Fmoc-2F-Phe-DAP (2F).....	page S10
Figure S4. High-resolution mass spectrum of Fmoc-2F-Phe-DAP (2F).....	page S11
Figure S5. ¹ H NMR spectrum of Fmoc-2Cl-Phe-DAP (2Cl).....	page S12
Figure S6. ¹³ C NMR spectrum of Fmoc-2Cl-Phe-DAP (2Cl).....	page S13
Figure S7. High-resolution mass spectrum of Fmoc-2Cl-Phe-DAP (2Cl).....	page S14
Figure S8. ¹ H NMR spectrum of Fmoc-2Br-Phe-DAP (2Br).....	page S15
Figure S9. ¹³ C NMR spectrum of Fmoc-2Br-Phe-DAP (2Br).....	page S16
Figure S10. High-resolution mass spectrum of Fmoc-2Br-Phe-DAP (2Br).....	page S17
Figure S11. ¹ H NMR spectrum of Fmoc-3Cl-Phe-DAP (3Cl).....	page S18
Figure S12. ¹³ C NMR spectrum of Fmoc-3Cl-Phe-DAP (3Cl).....	page S19
Figure S13. High-resolution mass spectrum of Fmoc-3Cl-Phe-DAP (3Cl).....	page S20
Figure S14. ¹ H NMR spectrum of Fmoc-3Br-Phe-DAP (3Br).....	page S21
Figure S15. ¹³ C NMR spectrum of Fmoc-3Br-Phe-DAP (3Br).....	page S22
Figure S16. High-resolution mass spectrum of Fmoc-3Br-Phe-DAP (3Br).....	page S23
Figure S17. ¹ H NMR spectrum of Fmoc-4F-Phe-DAP (4F).....	page S24
Figure S18. ¹³ C NMR spectrum of Fmoc-4F-Phe-DAP (4F).....	page S25
Figure S19. ¹⁹ F NMR spectrum of Fmoc-4F-Phe-DAP (4F).....	page S26
Figure S20. High-resolution mass spectrum of Fmoc-4F-Phe-DAP (4F).....	page S27
Figure S21. ¹ H NMR spectrum of Fmoc-4Cl-Phe-DAP (4Cl).....	page S28
Figure S22. ¹³ C NMR spectrum of Fmoc-4Cl-Phe-DAP (4Cl).....	page S29
Figure S23. High-resolution mass spectrum of Fmoc-4Cl-Phe-DAP (4Cl).....	page S30
Figure S24. ¹ H NMR spectrum of Fmoc-4Br-Phe-DAP (4Br).....	page S31
Figure S25. ¹³ C NMR spectrum of Fmoc-4Br-Phe-DAP (4Br).....	page S32
Figure S26. High-resolution mass spectrum of Fmoc-4Br-Phe-DAP (4Br).....	page S33
Figure S27. Analytical HPLC traces of compounds 2X–4X	page S34
Table S1. Analytical HPLC method conditions.....	page S34

Figure S28. TEM and digital images of compounds **2X–4X** one week after assembly.....page S35
Figure S29. Distribution of nanotubes in assemblies of Fmoc-4Cl-Phe-DAP (**4Cl**).....page S35
Figure S30. Strain sweep data for compounds **2X–4X**.....page S36
Figure S31. Frequency sweep data for compounds **2X–4X**.....page S37
References.....page S38

Scheme S1. Synthesis of Fmoc-X-Phe-DAP derivatives **2X–4X**.



The synthesis of Fmoc-X-Phe-Dap derivatives **2X–4X** was completed using the strategy outlined in **Scheme S1**, a slightly modified version of our previously reported synthetic method.¹ Details for the preparation of **2F** are provided as a representative example. Characterization data for **3F** may be found in a prior report.²



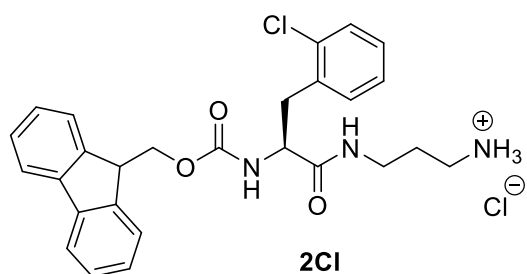
Fmoc-2F-Phe-DAP (2F):

Fmoc-2F-Phe-OH (0.2617 g, 0.65 mmol) and hydroxybenzotriazole (HOBt) (0.1260 g, 0.93 mmol) were dissolved in 2.5 mL of dichloromethane/dimethylformamide (1:1 DCM/DMF) and cooled in an ice bath while stirring. Then, *tert*-butyl *N*-(3-aminopropyl)carbamate (0.125 g, 0.72 mmol) was dissolved in 2.5 mL of 1:1 DCM/DMF and added to the reaction flask. 1-ethyl-3-(3-dimethylaminopropyl)carbodiimide hydrochloride (EDC·HCl) (0.1237 g, 0.65 mmol) was

dissolved in 5 mL of 1:1 DCM/DMF and added dropwise to the reaction mixture at a rate of approximately 1 drop every few seconds using a dropper funnel, then the mixture was left to stir overnight at room temperature. The following day, the mixture was concentrated by rotary evaporation to remove DCM, then diluted with 25 mL of ethyl acetate and washed twice with 25 mL of each of the following solutions: 5% aqueous acetic acid, 10% aqueous sodium bicarbonate, and saturated brine. The organic layer was dried over anhydrous sodium sulfate, which was removed by filtration. The resulting solution was concentrated by rotary evaporation to yield the crude product, which was purified using column chromatography (silica gel, ethyl acetate/hexanes) to yield a white solid (0.2344 g, 0.42 mmol, 65% yield).

The product obtained from purification (0.2344 g, 0.42 mmol) was dissolved in 10 mL of dichloromethane/methanol (3:1 DCM/MeOH). Then, 5.2 mL of 4 M HCl in dioxane (20.9 mmol) was added to the reaction mixture and it was stirred at room temperature for 30 minutes. The solution was poured into a 50 mL centrifuge tube and concentrated by rotary evaporation until there was about 5 mL of solution in the tube. Cold diethyl ether (20 mL) was added to precipitate the product, the tube was centrifuged for 10 minutes, and the supernatant was discarded. The pellet was resuspended in another 20 mL of cold diethyl ether, centrifuged, and decanted two more times for a total of three washes. The pellet was dried under vacuum to yield the desired product **2F** as a white solid (0.1945 g, 0.39 mmol, 94% yield, 61% yield across all steps).

^1H NMR (500 MHz, DMSO- d_6): δ 8.21 (t, $J = 5.1$ Hz, 1H), 8.00 (broad s, 3H), 7.88 (d, $J = 7.5$ Hz, 2H), (d, $J = 8.5$ Hz, 1H), 7.65 (t, $J = 8.5$ Hz, 2H), 7.45–7.37 (m, 2H), 7.36–7.03 (m, 6H), 4.33–4.07 (m, 4H), 3.22–3.02 (m, 3H), 2.86 (dd, $J = 12.8$ Hz, 10.1 Hz, 1H), 2.77–2.65 (m, 2H), 1.75–1.61 (m, 2H) ppm; ^{13}C NMR (125 MHz, DMSO- d_6): δ 173.4, 161.9 (d, $J = 243$ Hz), 156.9, 144.9, 141.8, 132.9, 129.7 (d, $J = 8.1$ Hz), 128.8, 126.5 (d, $J = 15.5$ Hz), 125.8 (d, $J = 15.1$ Hz), 125.2, 121.3, 116.2 (d, $J = 21.6$ Hz), 66.9, 60.0, 47.7, 37.7, 36.9, 32.1, 28.3 ppm; ^{19}F NMR (376 MHz, DMSO- d_6): δ -117.91–118.10 (m) ppm; HRMS (ESI-TOF) (m/z) 462.2175 (462.2187 calcd for $\text{C}_{27}\text{H}_{29}\text{FN}_3\text{O}_3$ [M] $^+$).

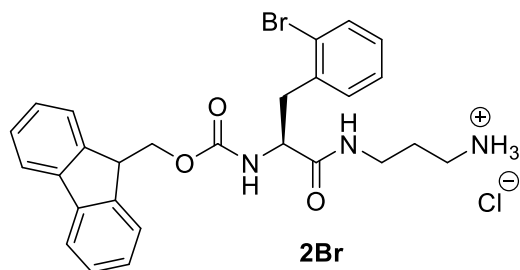


Fmoc-2Cl-Phe-DAP (2Cl):

The product **2Cl** was synthesized by the method above starting from Fmoc-2Cl-Phe-OH (0.2724 g, 0.65 mmol) and was recovered as a white solid (0.3027 g, 0.59 mmol, 91% yield).

^1H NMR (500 MHz, DMSO- d_6): δ 8.23–8.14 (m, 1H), 7.98 (broad s, 3H), 7.88 (d, $J = 7.4$ Hz, 2H), 7.79 (d, $J = 8.5$ Hz, 1H), 7.65 (dd, $J = 12.5$ Hz, 7.6 Hz, 2H), 7.45–7.26 (m, 6H), 7.21 (quintet, $J =$

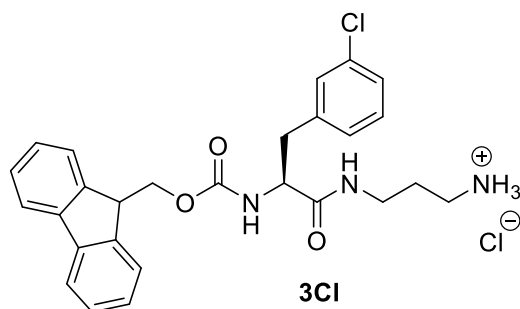
7.2 Hz, 2H), 4.40–4.05 (m, 4H), 3.24–3.07 (m, 3H), 2.94 (dd, $J = 12.4$ Hz, 10.2 Hz, 1H), 2.79–2.66 (m, 2H), 1.77–1.61 (m, 2H) ppm; ^{13}C NMR (125 MHz, DMSO- d_6): δ 172.4, 156.9, 144.9 (d, $J = 4.1$ Hz), 141.9, 136.5, 134.6, 132.8, 130.3, 129.6, 128.8, 128.2 (d, $J = 21.9$ Hz), 126.5 (d, $J = 12.9$ Hz), 121.3, 66.9, 55.4, 47.7, 37.7, 36.9, 36.4, 28.3 ppm; HRMS (ESI-TOF) (m/z) 478.1884 (478.1892 calcd for $\text{C}_{27}\text{H}_{29}\text{ClN}_3\text{O}_3$ [M] $^+$).



Fmoc-2Br-Phe-DAP (2Br):

The product **2Br** was synthesized by the method above starting from Fmoc-2Br-Phe-OH (0.3010 g, 0.65 mmol) and was recovered as a white solid (0.2949 g, 0.53 mmol, 82% yield).

^1H NMR (500 MHz, DMSO- d_6): δ 8.15 (t, $J = 5.1$ Hz, 1H), 8.00 (broad s, 3H), 7.88 (d, $J = 7.5$ Hz, 2H), 7.80 (d, $J = 8.6$ Hz, 1H), 7.67 (dd, $J = 12.5$ Hz, 7.6 Hz, 2H), 7.57 (d, $J = 8.0$ Hz, 1H), 7.45–7.27 (m, 5H), 7.24 (t, $J = 7.4$ Hz, 1H), 7.14 (t, $J = 7.6$ Hz, 1H), 4.42–4.05 (m, 4H), 3.24–3.07 (m, 3H), 2.95 (dd, $J = 13.1$ Hz, 10.1 Hz, 1H), 2.80–2.67 (m, 2H), 1.78–1.63 (m, 2H) ppm; ^{13}C NMR (125 MHz, DMSO- d_6): δ 172.3, 156.9, 144.9 (d, $J = 5.3$ Hz), 141.9, 138.2, 133.6, 132.8, 129.8, 128.8, 128.6, 128.2, 126.5 (d, $J = 12.1$ Hz), 121.3, 66.9, 55.5, 47.7, 38.8, 37.7, 36.9, 28.2 ppm; HRMS (ESI-TOF) (m/z) 522.1382 (522.1387 calcd for $\text{C}_{27}\text{H}_{29}\text{BrN}_3\text{O}_3$ [M] $^+$).

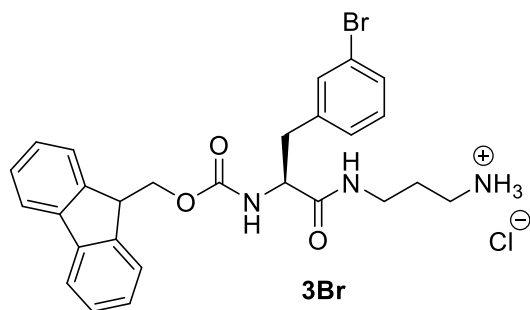


Fmoc-3Cl-Phe-DAP (3Cl):

The product **3Cl** was synthesized by the method above starting from Fmoc-3Cl-Phe-OH (0.2724 g, 0.65 mmol) and was recovered as a white solid (0.2361 g, 0.46 mmol, 71% yield).

^1H NMR (500 MHz, DMSO- d_6): δ 8.38–8.31 (m, 1H), 8.02 (broad s, 3H), 7.88 (d, $J = 7.4$ Hz, 2H), 7.75 (d, $J = 8.4$ Hz, 1H), 7.63 (t, $J = 8.7$ Hz, 2H), 7.51–7.22 (m, 8H), 4.29–4.04 (m, 4H), 3.21–3.08 (m, 2H), 3.05–2.94 (m, 1H), 2.86–2.69 (m, 3H), 1.79–1.63 (m, 2H) ppm; ^{13}C NMR (125 MHz, DMSO- d_6): δ 172.7, 157.0, 144.9 (d, $J = 7.6$ Hz), 141.9 (d, $J = 21.5$ Hz), 133.9, 131.1, 130.3,

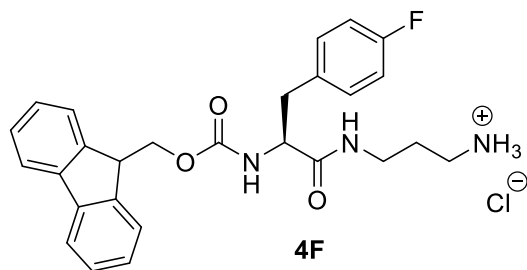
129.2, 128.8, 128.2, 127.5, 126.5 (d, $J = 14.5$ Hz), 121.3, 66.9, 57.4, 47.7, 38.3, 37.8, 36.9, 28.4 ppm; HRMS (ESI-TOF) (m/z) 478.1884 (478.1892 calcd for $C_{27}H_{29}ClN_3O_3 [M]^+$).



Fmoc-3Br-Phe-DAP (**3Br**):

The product **3Br** was synthesized by the method above starting from Fmoc-3Br-Phe-OH (0.3010 g, 0.65 mmol) and was recovered as a white solid (0.2222 g, 0.40 mmol, 62% yield).

1H NMR (500 MHz, DMSO- d_6): δ 8.32 (t, $J = 5.1$ Hz, 1H), 7.98 (broad s, 3H), 7.88 (d, $J = 7.5$ Hz, 2H), 7.74 (d, $J = 8.4$ Hz, 1H), 7.63 (t, $J = 9.0$ Hz, 2H), 7.56 (s, 1H), 7.45–7.19 (m, 7H), 4.28–4.05 (m, 4H), 3.15 (dt, $J = 6.1$ Hz, 5.8 Hz), 2.98 (dd, $J = 13.6$ Hz, 3.6 Hz), 2.86–2.69 (m, 3H), 1.78–1.64 (m, 2H) ppm; ^{13}C NMR (125 MHz, DMSO- d_6): δ 172.7, 157.0, 144.9 (d, $J = 7.4$ Hz), 142.3, 141.8, 133.1, 131.4, 130.4, 129.6, 128.8, 128.2, 126.5 (d, $J = 14.7$ Hz), 122.6, 121.3, 66.9, 57.4, 47.7, 38.3, 37.8, 36.9, 28.4 ppm; HRMS (ESI-TOF) (m/z) 522.1381 (522.1387 calcd for $C_{27}H_{29}BrN_3O_3 [M]^+$).

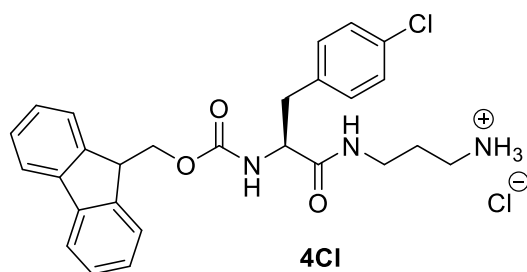


Fmoc-4F-Phe-DAP (**4F**):

The product **4F** was synthesized by the method above (scaled up) starting from Fmoc-4F-Phe-OH (2.30 g, 5.67 mmol) and was recovered as a white solid (1.90 g, 3.82 mmol, 67% yield).

1H NMR (500 MHz, DMSO- d_6): δ 8.29 (t, $J = 4.8$ Hz, 1H), 7.99 (broad s, 3H), 7.88 (d, $J = 7.5$ Hz, 2H), 7.68 (d, $J = 8.5$ Hz, 1H), 7.66–7.58 (m, 2H), 7.45–7.20 (m, 6H), 7.08 (t, $J = 8.4$ Hz, 2H), 4.23–4.06 (m, 4H), 3.14 (dt, $J = 6.0$ Hz, 6.0 Hz, 2H) 2.97 (dd, $J = 13.5$ Hz, 3.8 Hz, 1H), 2.85–2.68 (m, 3H), 1.77–1.63 (m, 2H) ppm; ^{13}C NMR (125 MHz, DMSO- d_6): δ 172.8, 162.1 (d, $J = 240$ Hz), 144.9 (d, $J = 11.8$ Hz), 141.9, 135.5, 132.2 (d, $J = 7.6$ Hz), 128.8, 128.2, 126.5 (d, $J = 9.3$ Hz), 121.3, 115.9 (d, $J = 20.8$ Hz), 66.8, 57.6, 47.7, 37.9, 37.8, 28.4 ppm; ^{19}F NMR (376 MHz, DMSO-

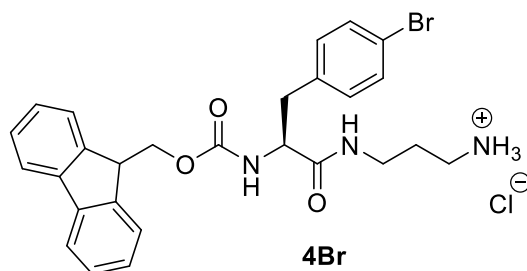
d₆): δ -116.94–117.08 (m) ppm; HRMS (ESI-TOF) (m/z) 462.2176 (462.2187 calcd for C₂₇H₂₉FN₃O₃ [M]⁺).



Fmoc-4Cl-Phe-DAP (4Cl):

The product **4Cl** was synthesized by the method above starting from Fmoc-4Cl-Phe-OH (0.2724 g, 0.65 mmol) and was recovered as a white solid (0.2315 g, 0.45 mmol, 70% yield).

¹H NMR (500 MHz, DMSO-d₆): δ 8.31 (t, J = 5.1 Hz, 1H), 7.97 (broad s, 3H), 7.88 (d, J = 7.5 Hz, 2H), 7.70 (d, J = 8.5 Hz, 1H), 7.63 (t, J = 7.0 Hz, 2H), 7.45–7.22 (m, 8H), 4.23–4.08 (m, 4H), 3.14 (dt, J = 5.9 Hz, 5.7 Hz), 2.97 (dd, J = 13.6 Hz, 3.5 Hz), 2.85–2.69 (m, 3H), 1.77–1.64 (m, 2H) ppm; ¹³C NMR (125 MHz, DMSO-d₆): δ 172.7, 160.0, 144.9 (d, J = 13.5 Hz), 141.9, 138.4, 132.3, 132.2, 129.2, 128.8, 128.2, 126.5 (d, J = 9.4 Hz), 121.3, 66.8, 57.4, 47.7, 38.0, 37.8, 36.9, 28.4 ppm; HRMS (ESI-TOF) (m/z) 478.1884 (478.1892 calcd for C₂₇H₂₉ClN₃O₃ [M]⁺).



Fmoc-4Br-Phe-DAP (4Br):

The product **4Br** was synthesized by the method above (scaled up) starting from Fmoc-4Br-Phe-OH (1.20 g, 2.58 mmol) and was recovered as a white solid (1.17 g, 2.09 mmol, 81% yield).

¹H NMR (500 MHz, DMSO-d₆): δ 8.33 (t, J = 5.1 Hz, 1H), 8.02 (broad s, 3H), 7.88 (d, J = 7.5 Hz, 2H), 7.69 (d, J = 8.5 Hz, 1H), 7.63 (t, J = 7.5 Hz, 2H), 7.48–7.20 (m, 8H), 4.25–4.05 (m, 4H), 3.15 (dt, J = 6.0 Hz, 5.6 Hz), 2.97 (dd, J = 13.7 Hz, 3.8 Hz, 1H), 2.83–2.69 (m, 3H), 1.79–1.63 (m, 2H) ppm; ¹³C NMR (125 MHz, DMSO-d₆): δ 172.7, 157.0, 144.9 (d, J = 14.2 Hz), 141.9, 138.8, 132.4 (d, J = 73.4 Hz), 128.5 (d, J = 73.8 Hz), 126.5 (d, J = 9.4 Hz), 121.3, 120.7, 66.8, 57.3, 47.7, 38.1, 37.8, 36.9, 28.4 ppm; HRMS (ESI-TOF) (m/z) 522.1381 (522.1387 calcd for C₂₇H₂₉BrN₃O₃ [M]⁺).

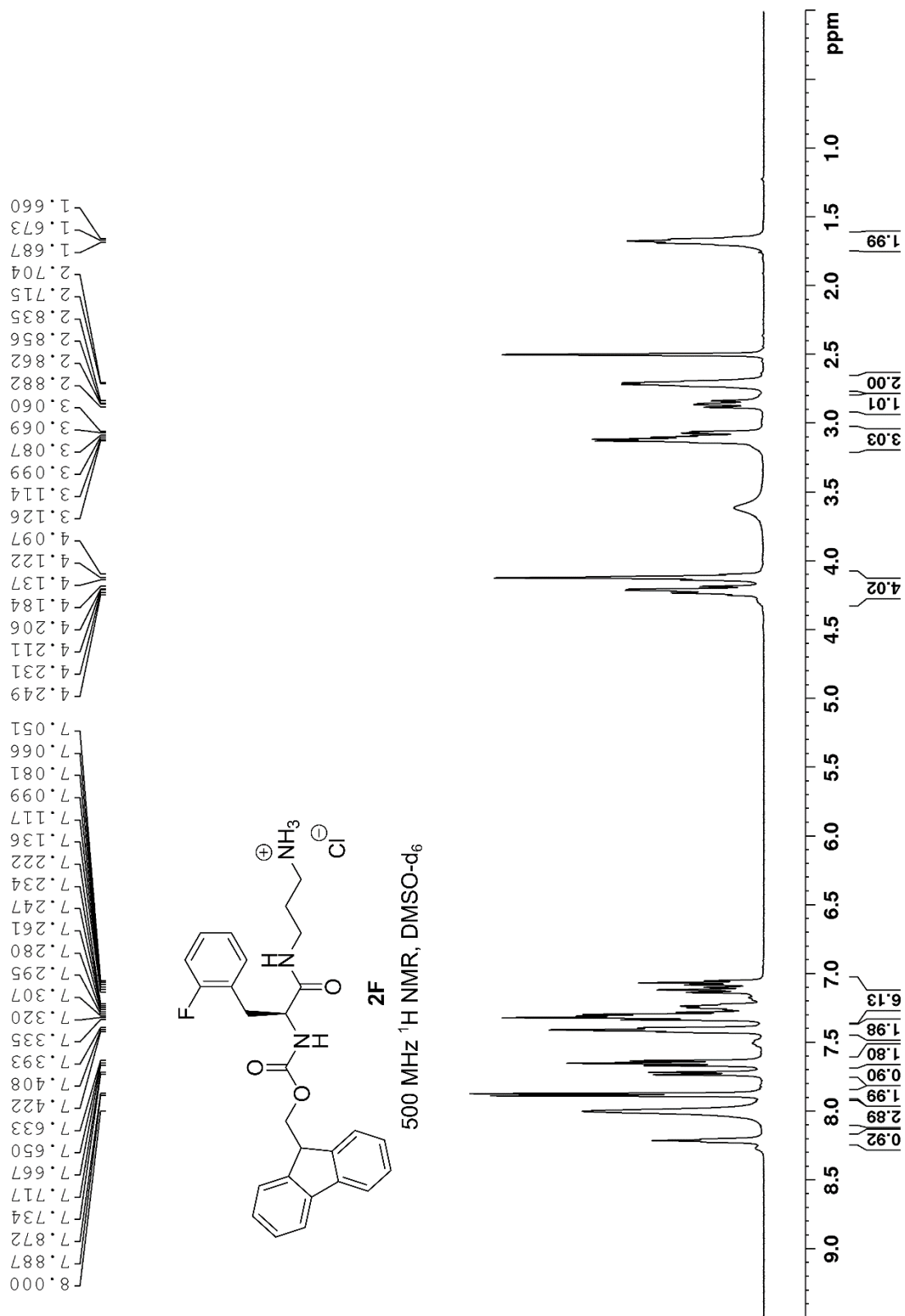


Figure S1. ¹H NMR spectrum of Fmoc-2F-Phe-DAP (**2F**).

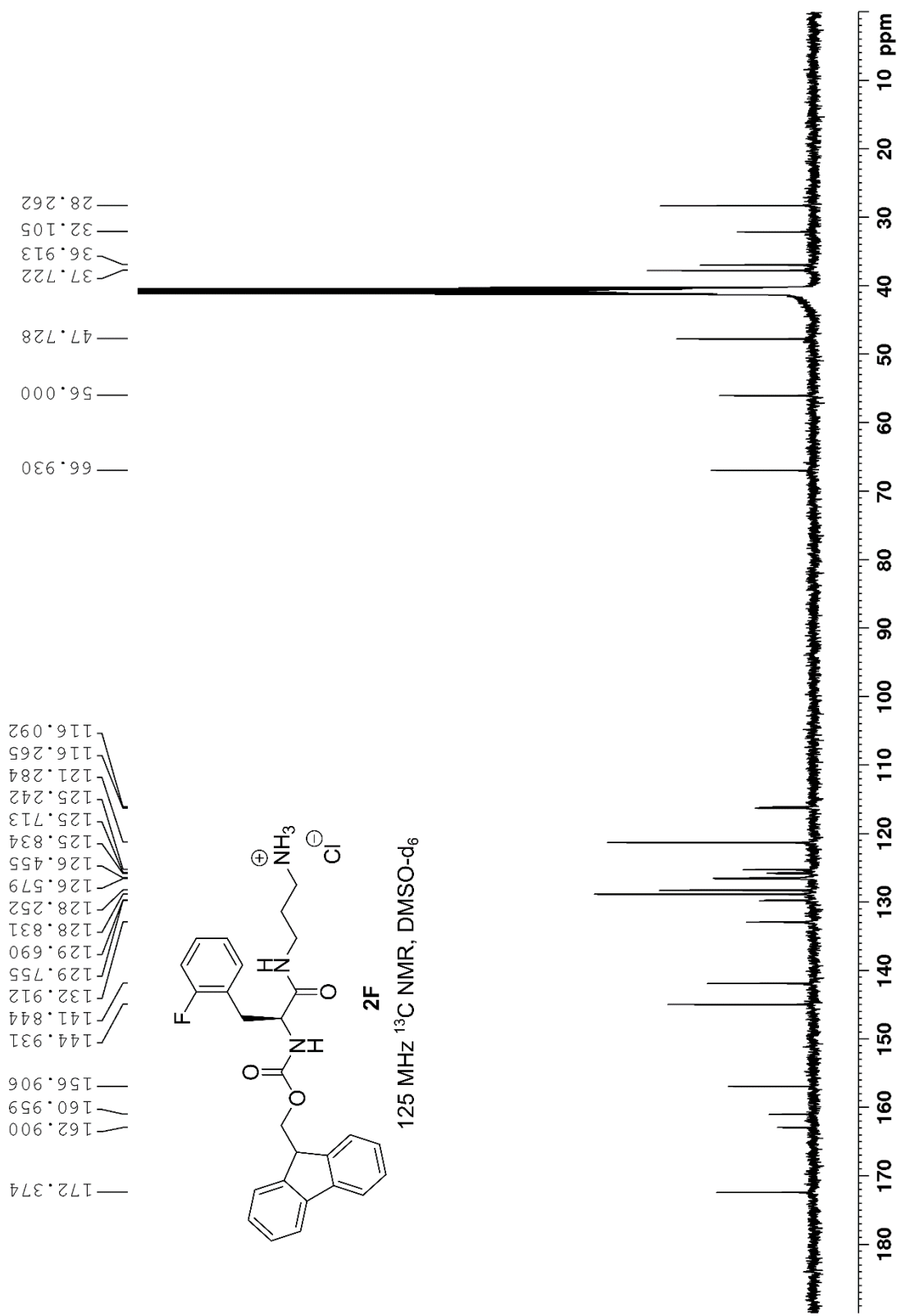


Figure S2. ^{13}C NMR spectrum of Fmoc-2F-Phe-DAP (**2F**).

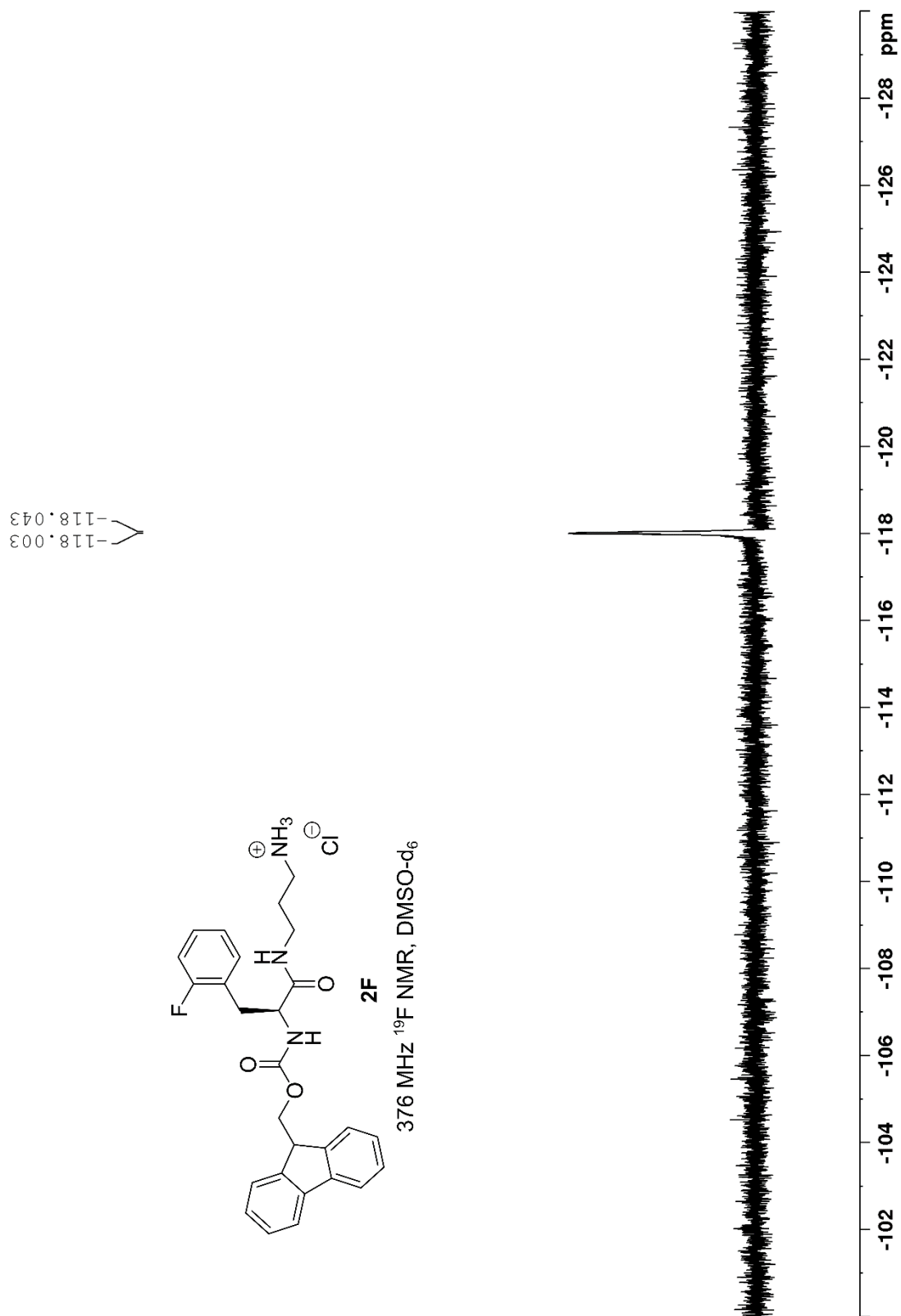


Figure S3. ^{19}F NMR spectrum of Fmoc-2F-Phe-DAP (**2F**).

2F #88-179 RT: 0.39-0.79 AV: 92 NL: 1.28E9
T: FTMS +p ESI Full ms [140.0000-1000.0000]

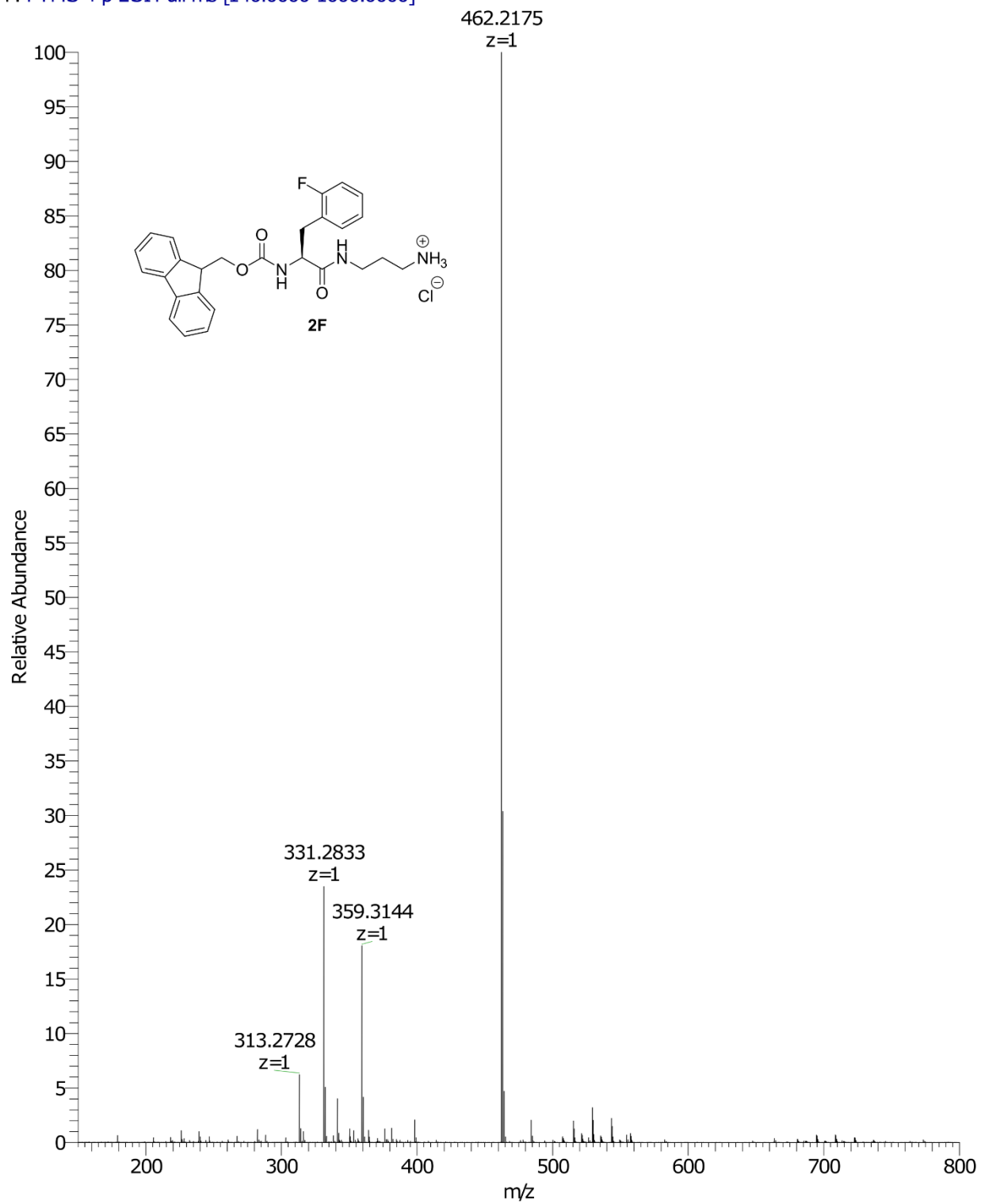


Figure S4. High-resolution mass spectrum of Fmoc-2F-Phe-DAP (2F).

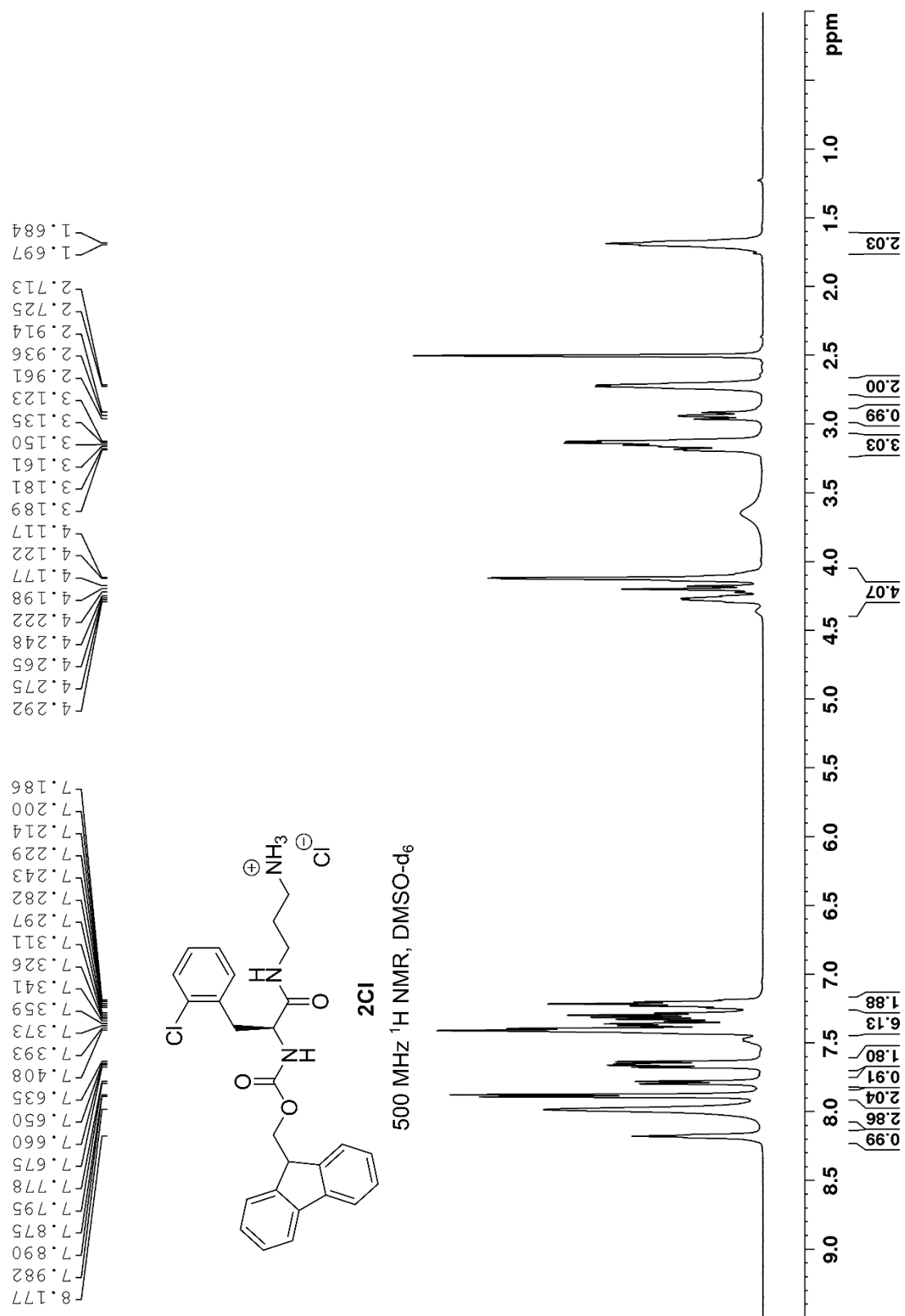


Figure S5. ^1H NMR spectrum of Fmoc-2Cl-Phe-DAP (**2Cl**).

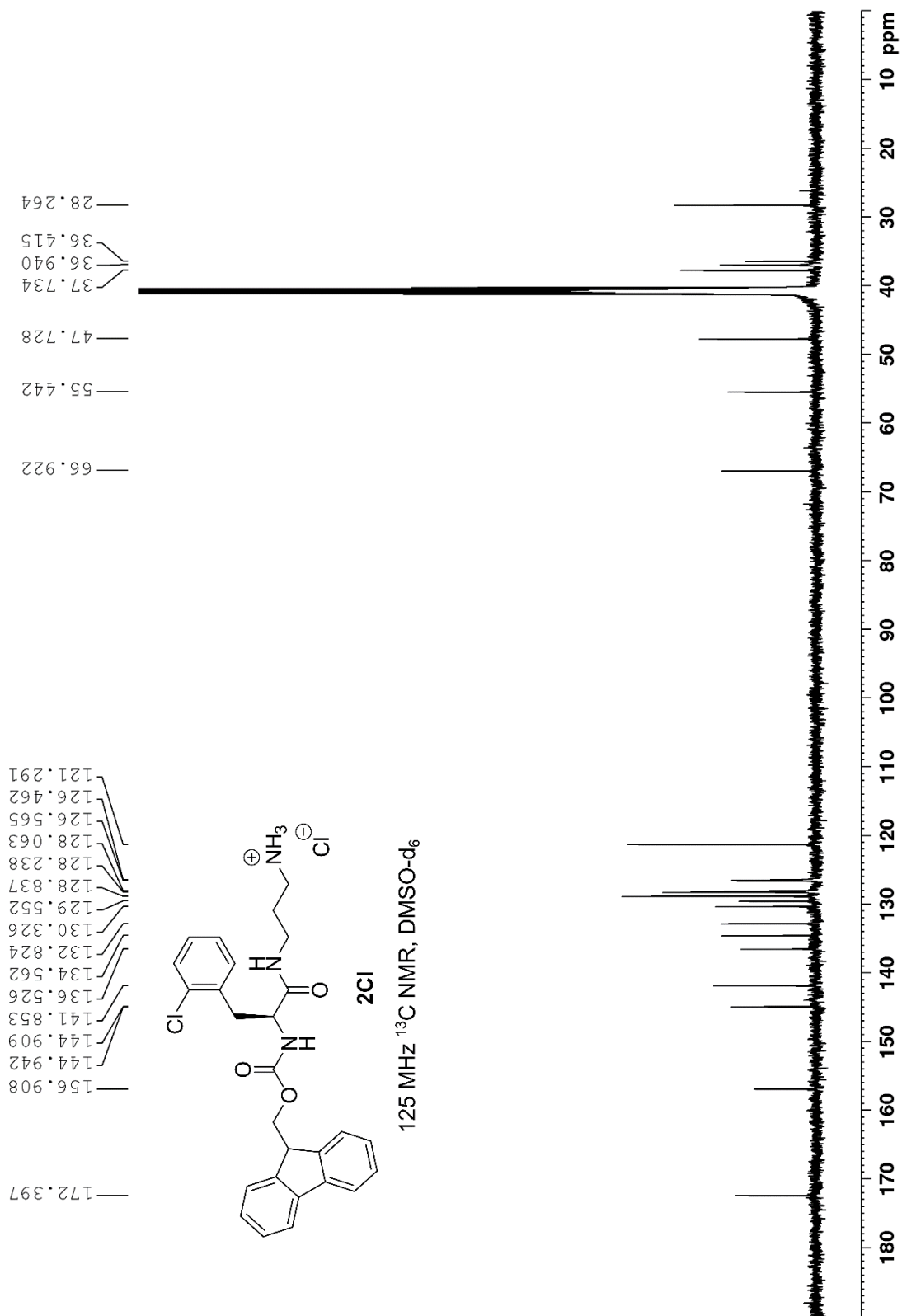


Figure S6. ¹³C NMR spectrum of Fmoc-2Cl-Phe-DAP (**2Cl**).

2Cl #89-182 RT: 0.39-0.80 AV: 94 NL: 9.44E8
T: FTMS +p ESI Full ms [140.0000-1000.0000]

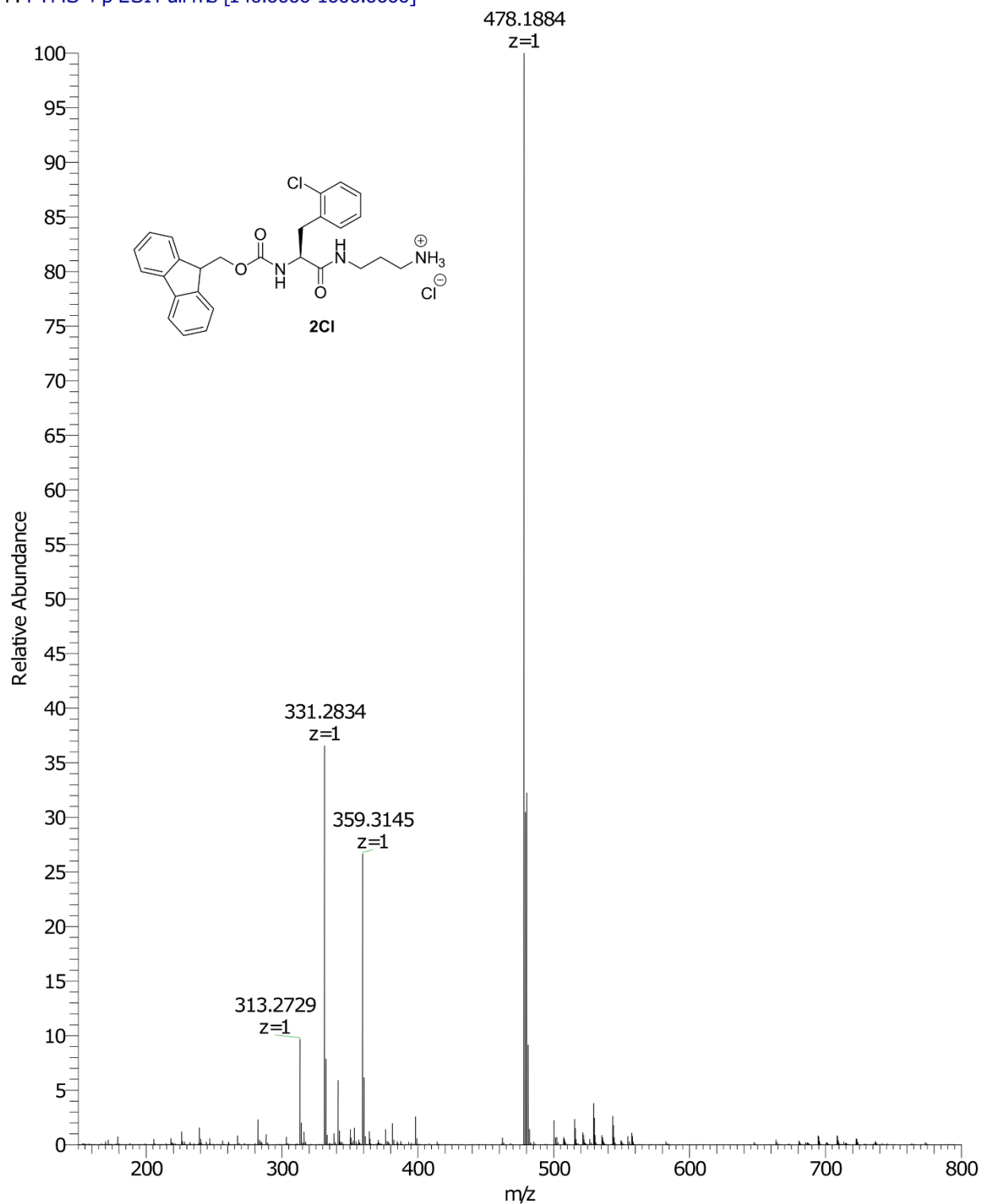


Figure S7. High-resolution mass spectrum of Fmoc-2Cl-Phe-DAP (2Cl).

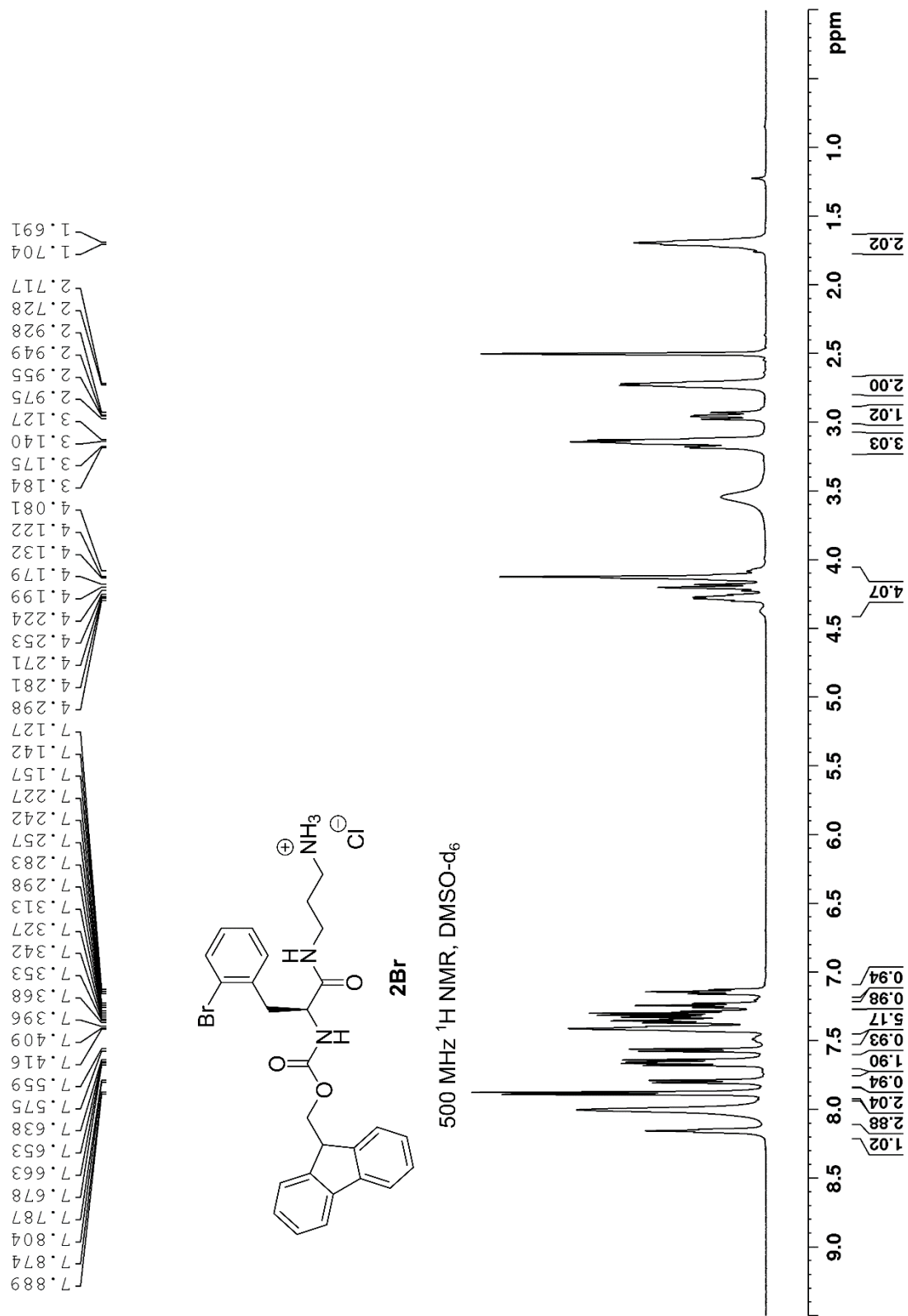


Figure S8. ¹H NMR spectrum of Fmoc-2Br-Phe-DAP (**2Br**).

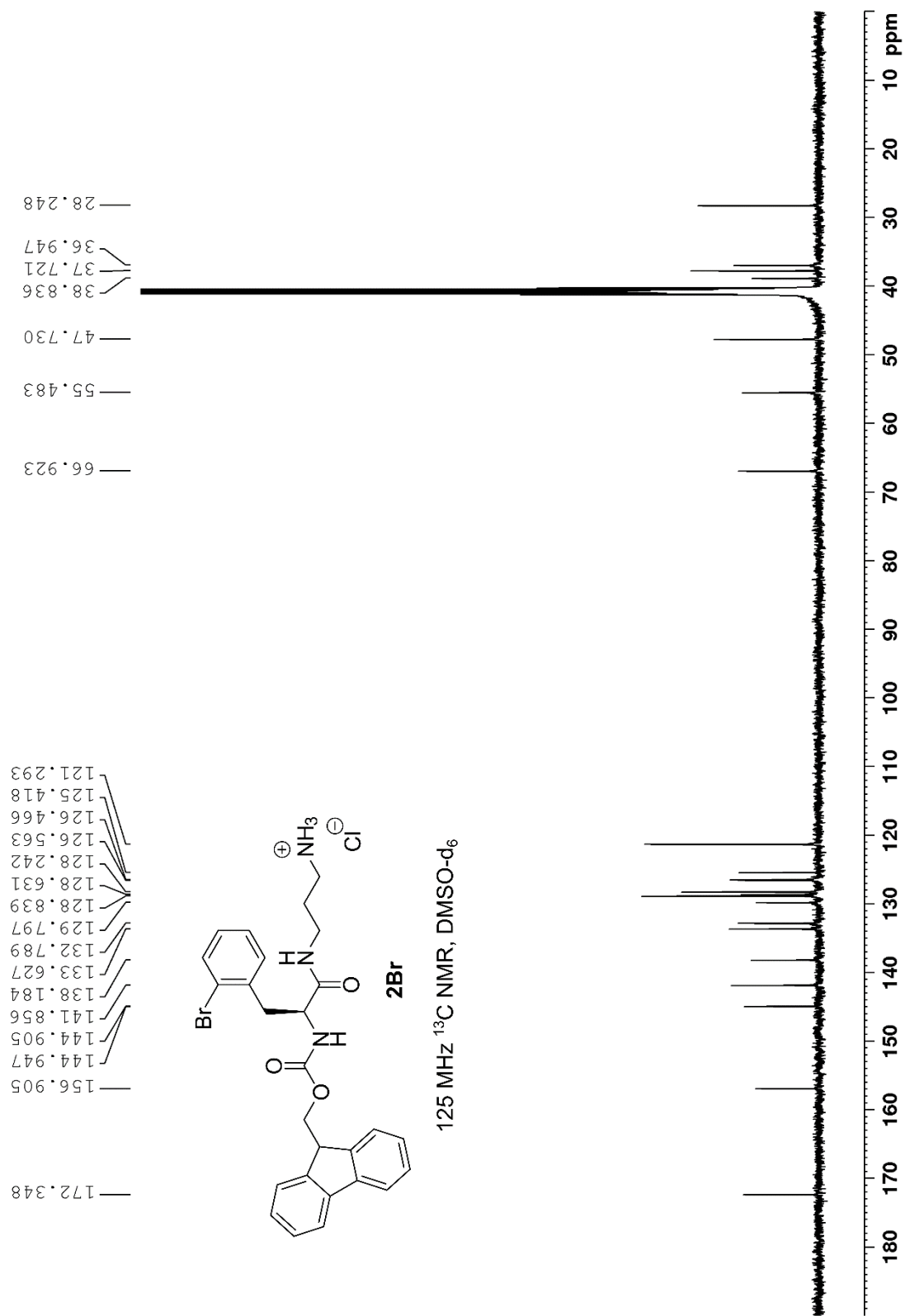


Figure S9. ¹³C NMR spectrum of Fmoc-2Br-Phe-DAP (**2Br**).

2Br #88-181 RT: 0.39-0.80 AV: 94 NL: 5.98E8
T: FTMS +p ESI Full ms [140.0000-1000.0000]

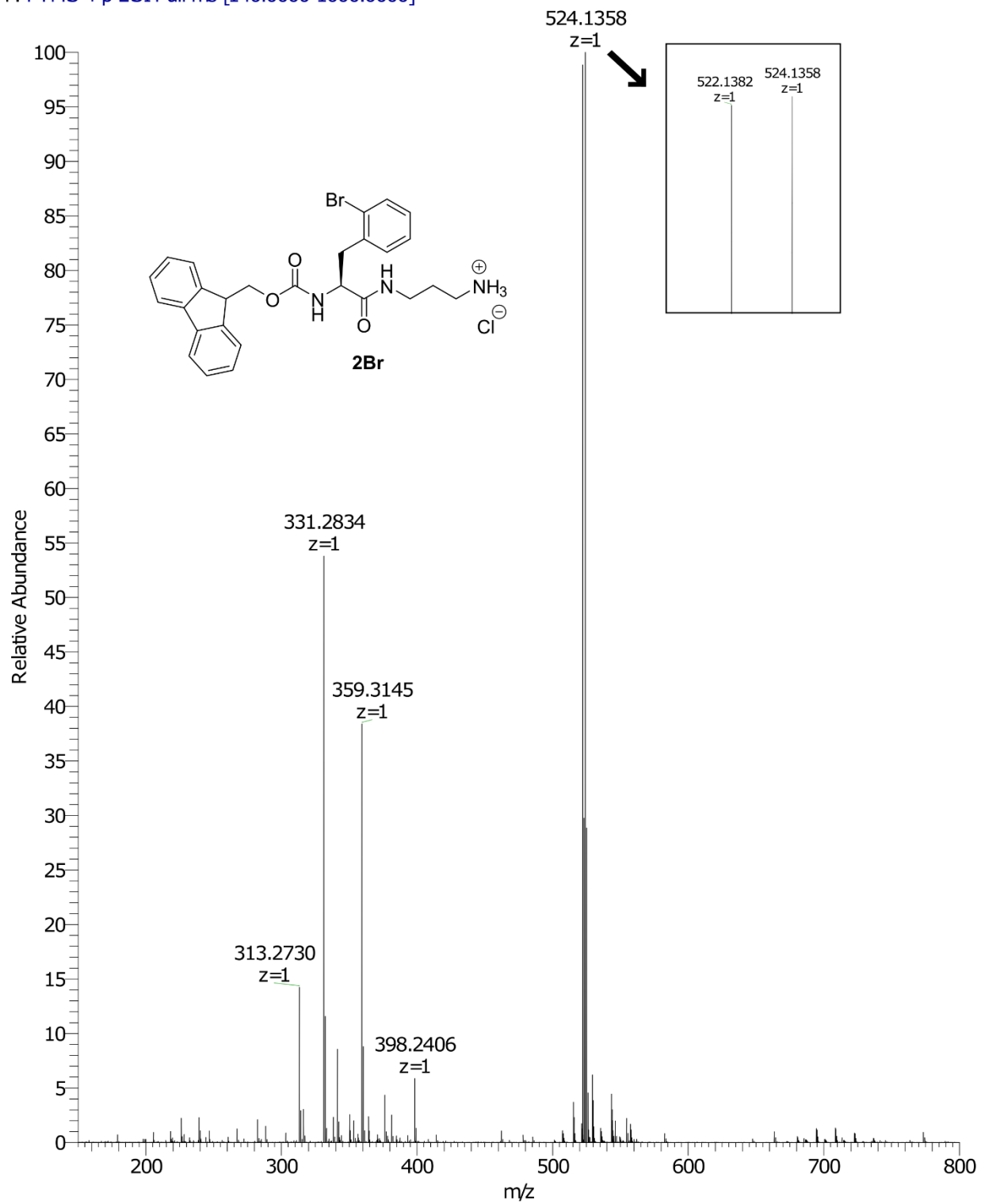


Figure S10. High-resolution mass spectrum of Fmoc-2Br-Phe-DAP (**2Br**).

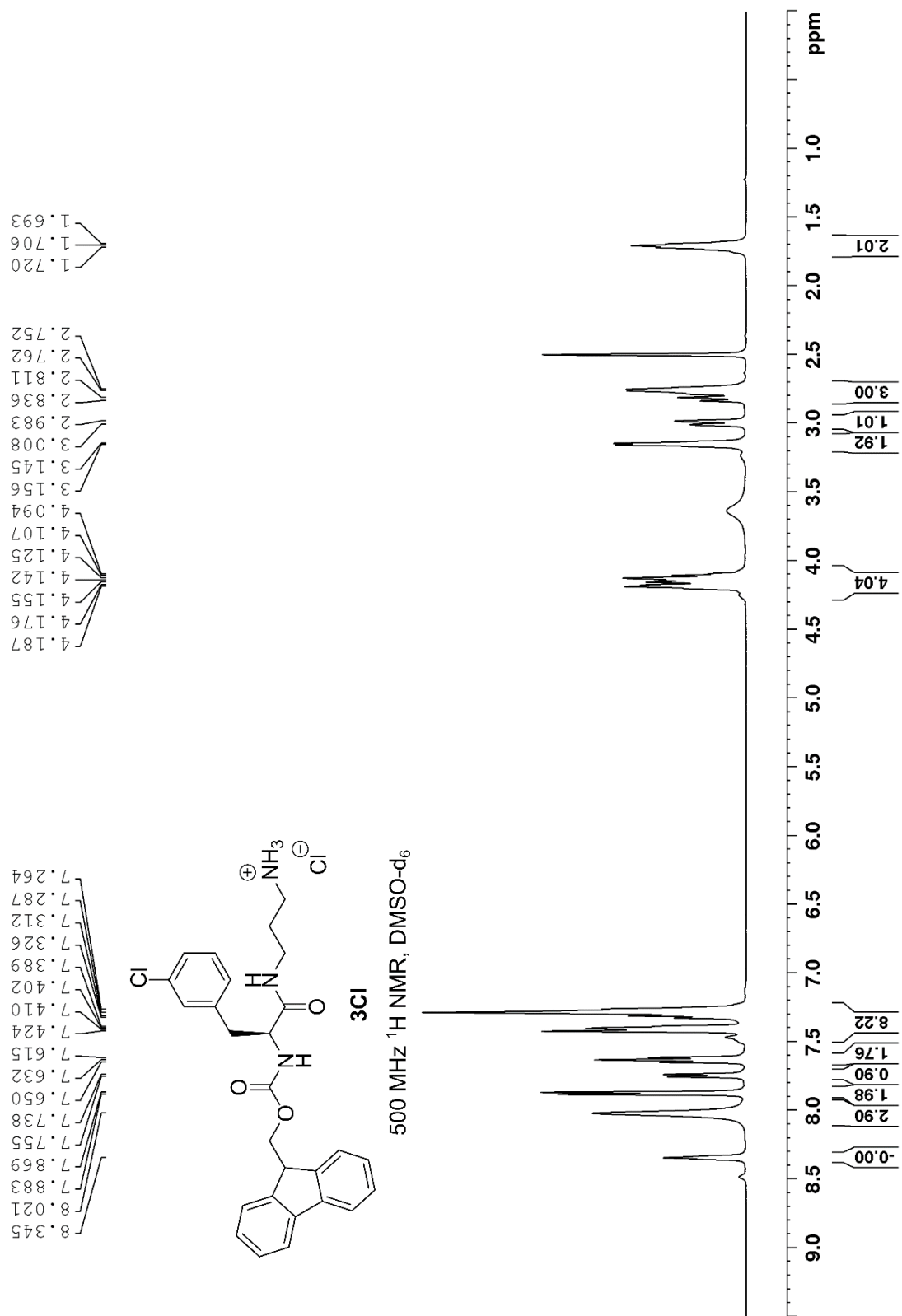


Figure S11. ^1H NMR spectrum of Fmoc-3Cl-Phe-DAP (**3Cl**).

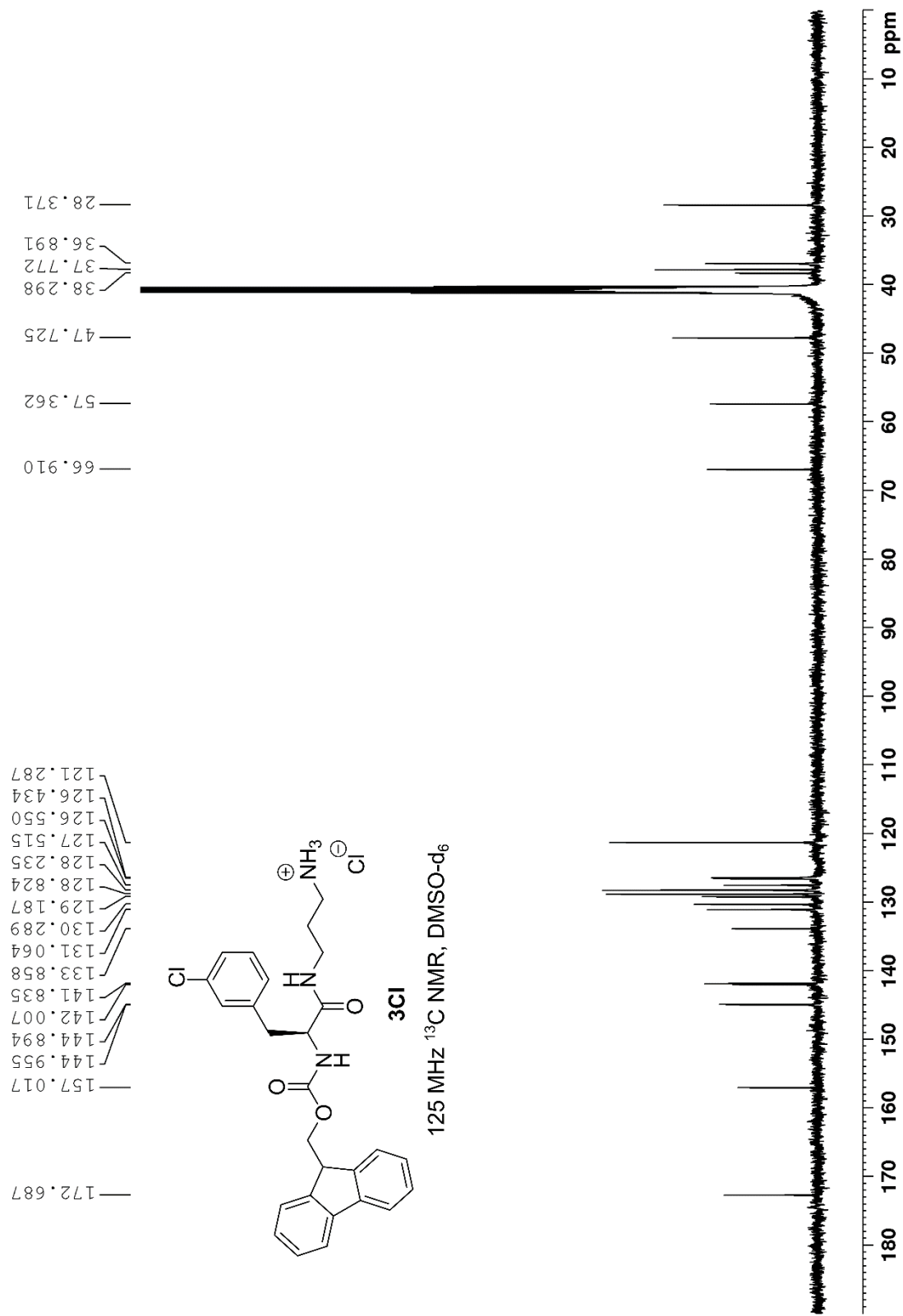


Figure S12. ^{13}C NMR spectrum of Fmoc-3Cl-Phe-DAP (**3Cl**).

3Cl #88-181 RT: 0.39-0.80 AV: 94 NL: 9.37E8
T: FTMS +p ESI Full ms [140.0000-1000.0000]

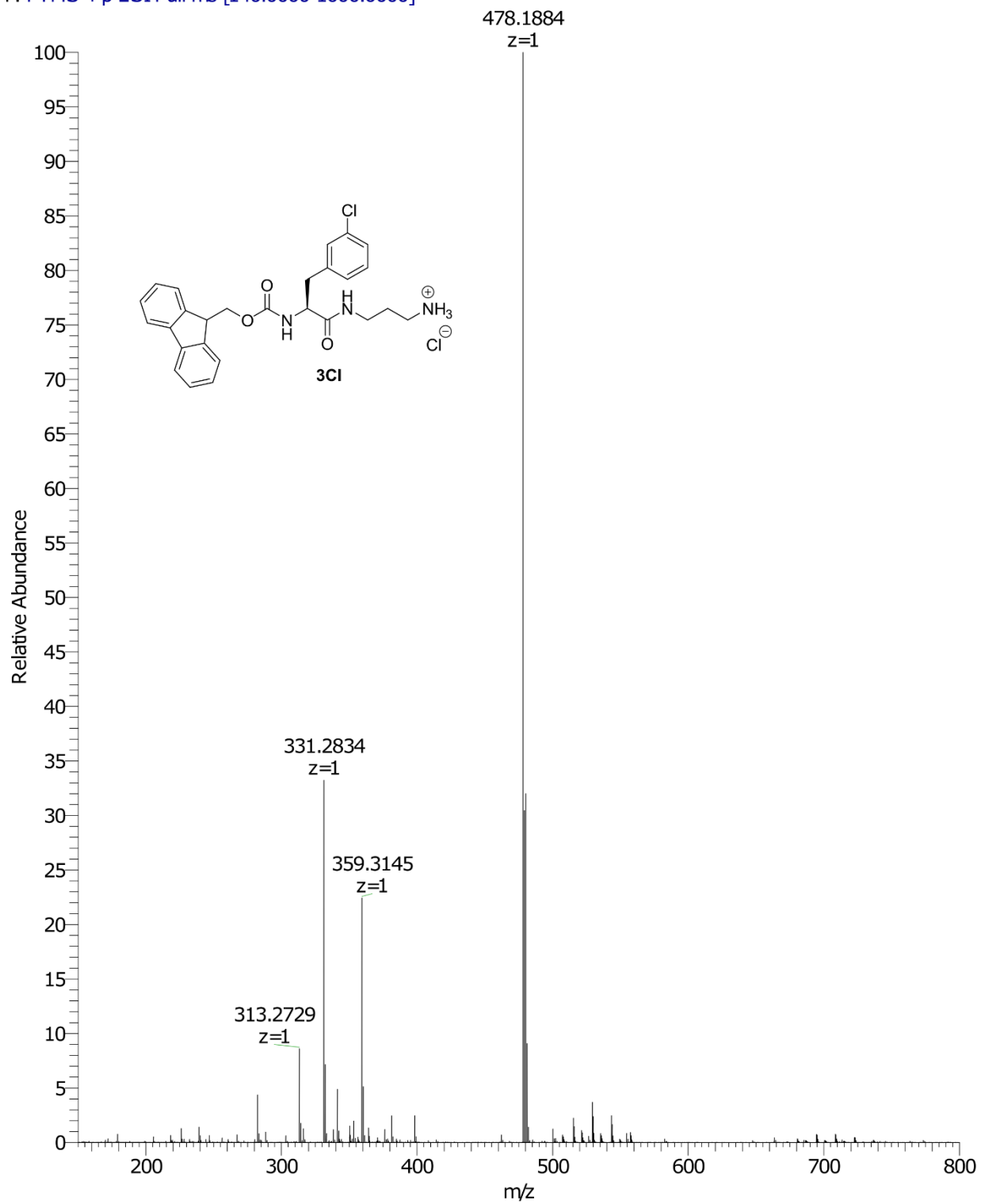


Figure S13. High-resolution mass spectrum of Fmoc-3Cl-Phe-DAP (**3Cl**).

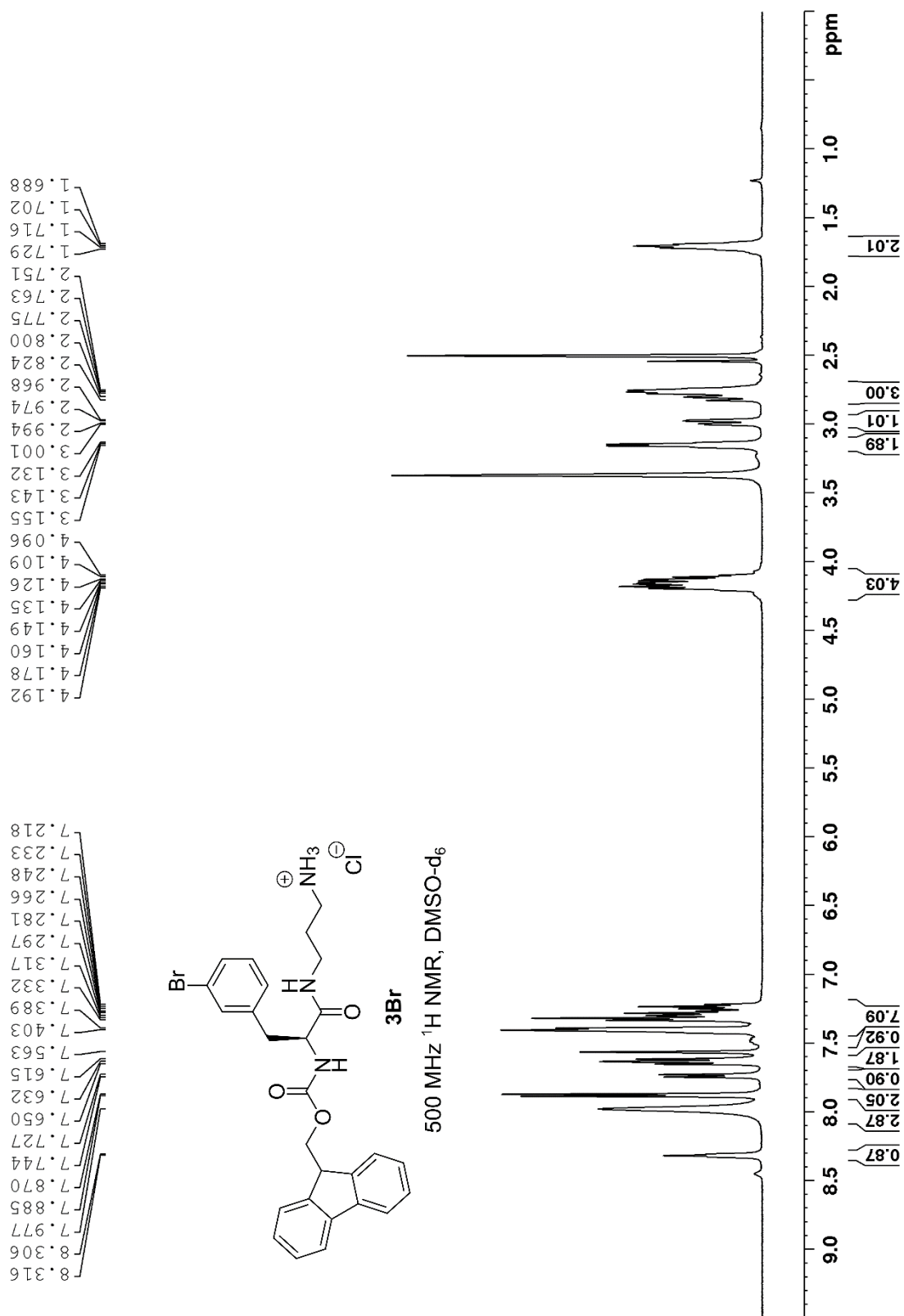


Figure S14. ¹H NMR spectrum of Fmoc-3Br-Phe-DAP (**3Br**).

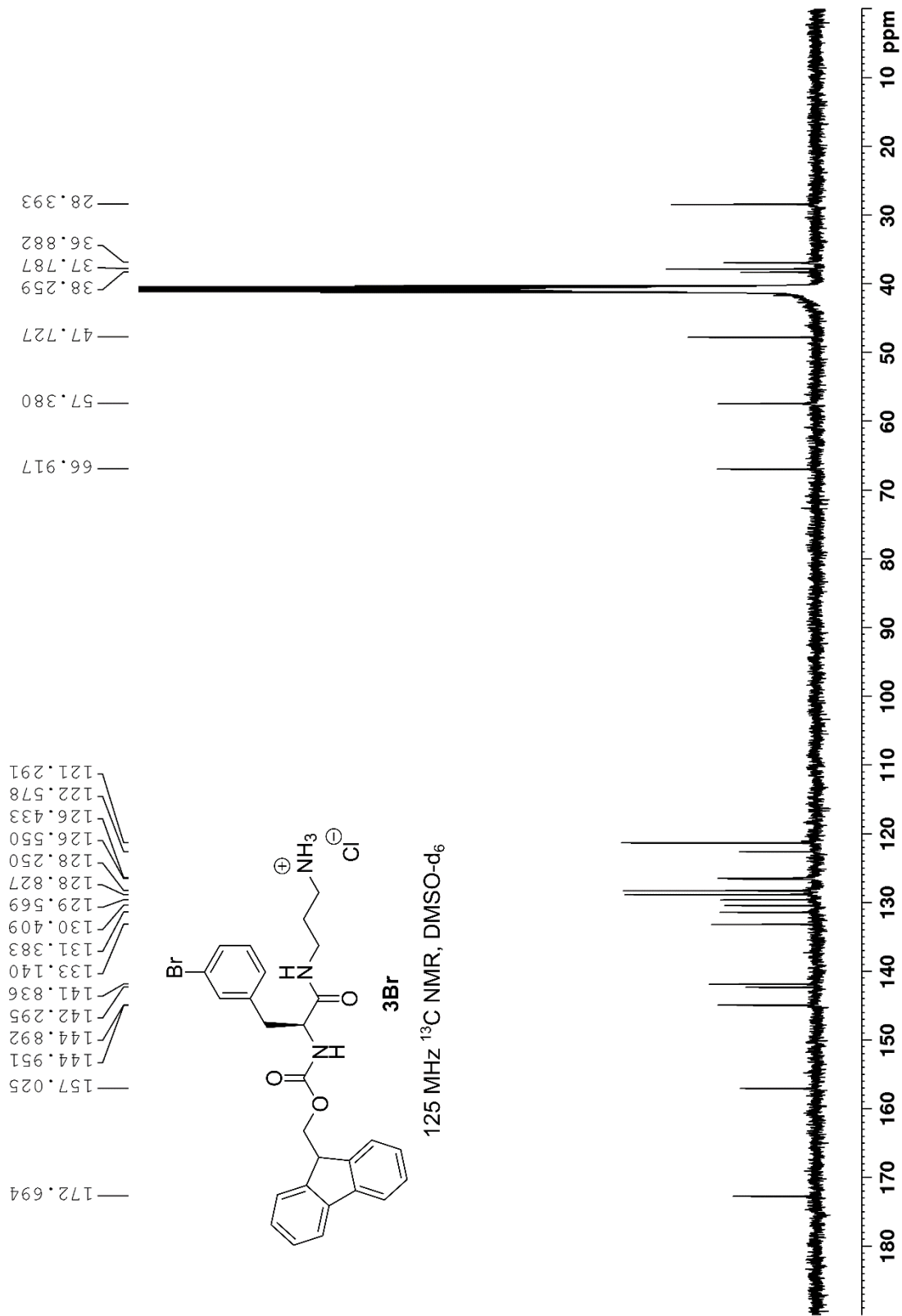


Figure S15. ^{13}C NMR spectrum of Fmoc-3Br-Phe-DAP (**3Br**).

3Br #88-181 RT: 0.39-0.80 AV: 94 NL: 6.65E8
T: FTMS +p ESI Full ms [140.0000-1000.0000]

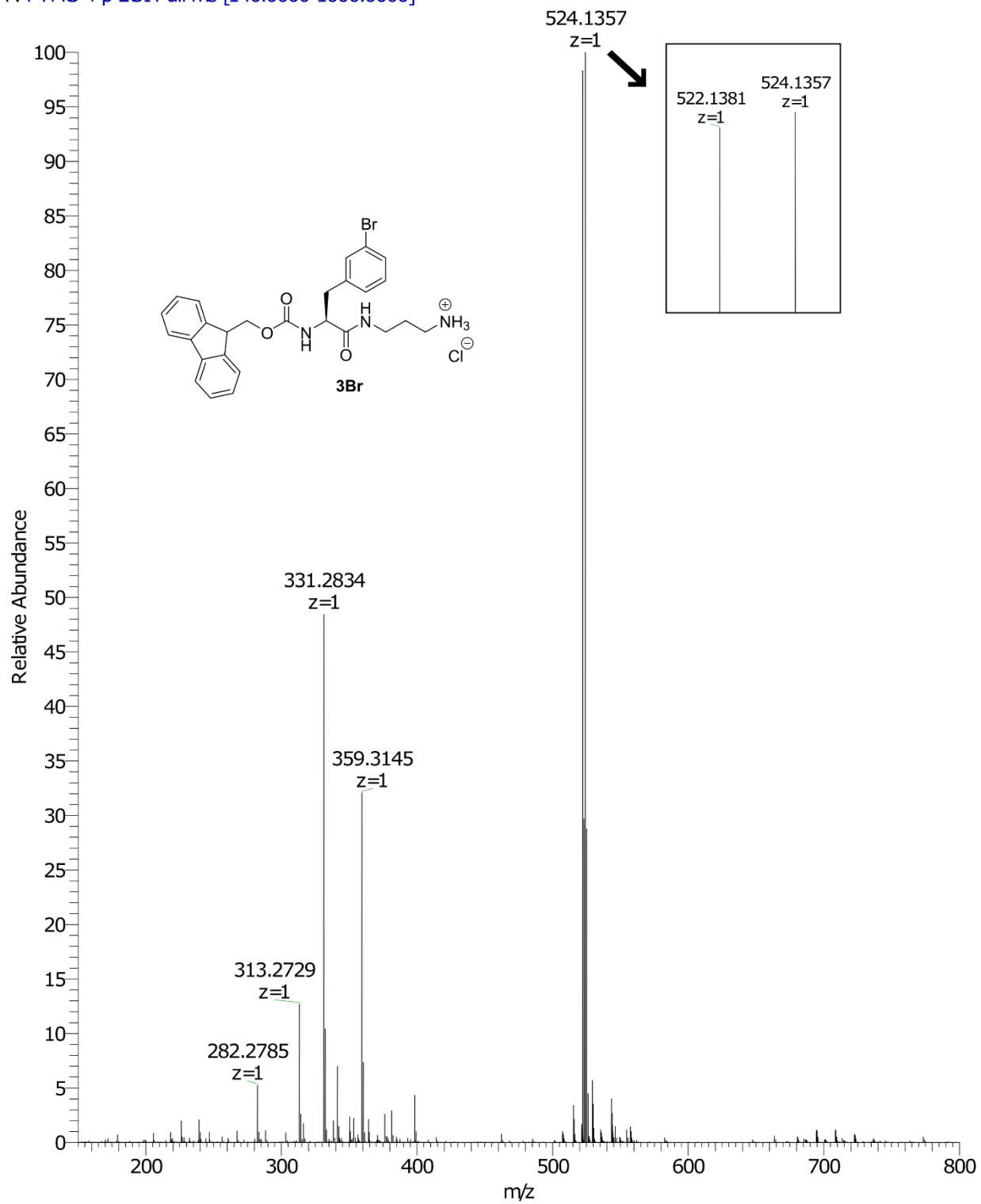


Figure S16. High-resolution mass spectrum of Fmoc-3Br-Phe-DAP (**3Br**).

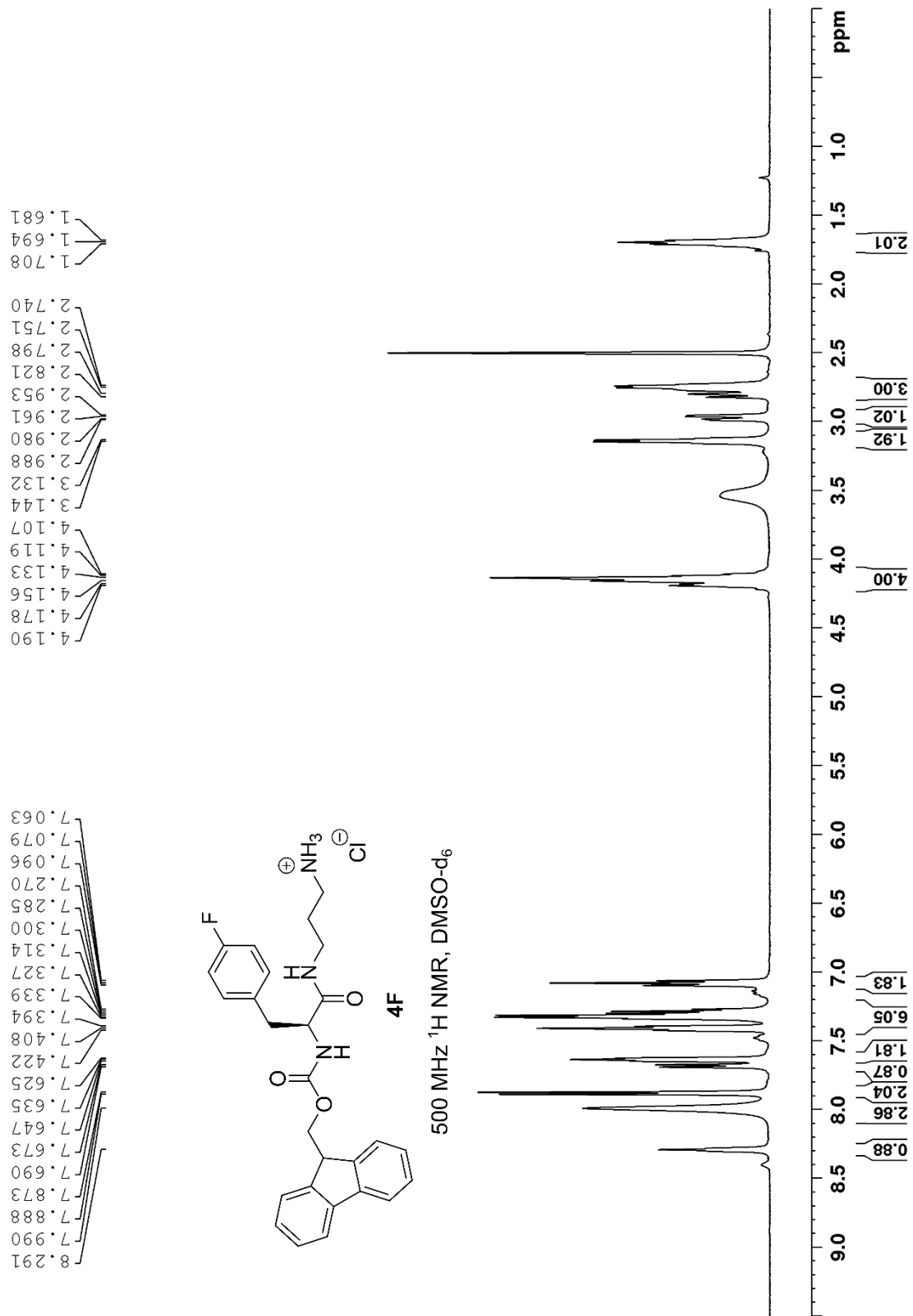


Figure S17. ¹H NMR spectrum of Fmoc-4F-Phe-DAP (**4F**).

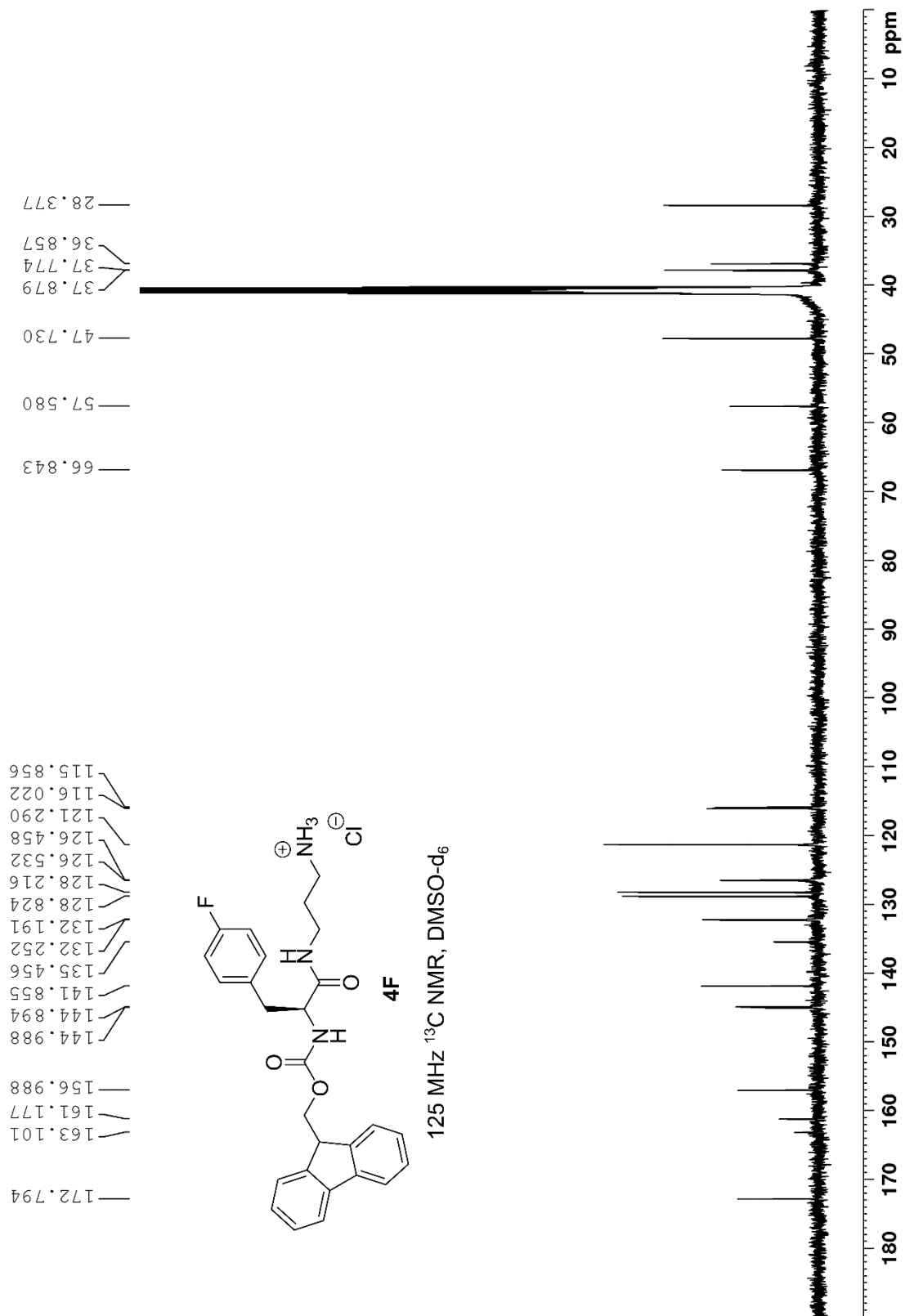


Figure S18. ^{13}C NMR spectrum of Fmoc-4F-Phe-DAP (4F).

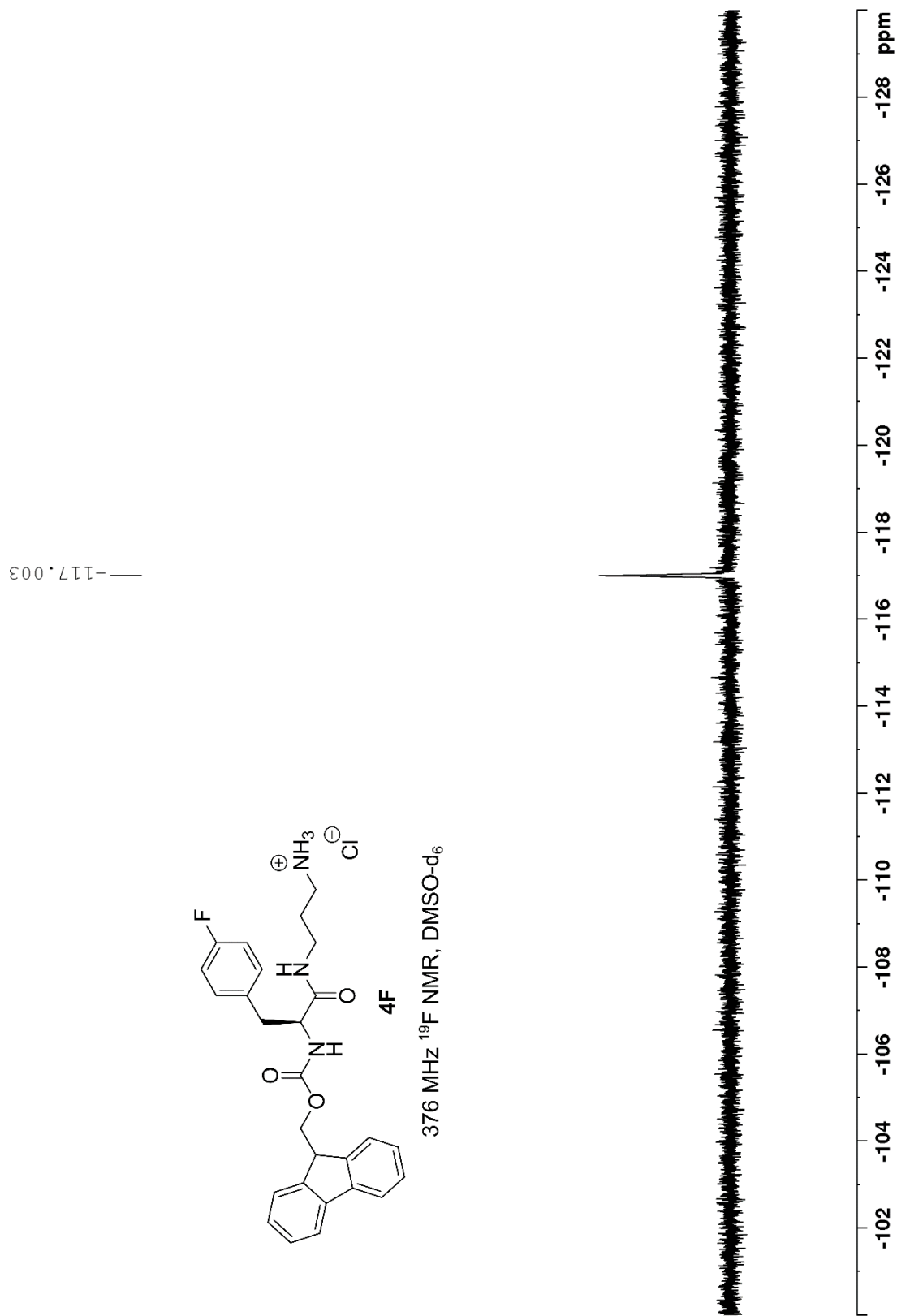


Figure S19. ^{19}F NMR spectrum of Fmoc-4F-Phe-DAP (**4F**).

4F #87-181 RT: 0.39-0.80 AV: 95 NL: 1.03E9
T: FTMS +p ESI Full ms [140.0000-1000.0000]

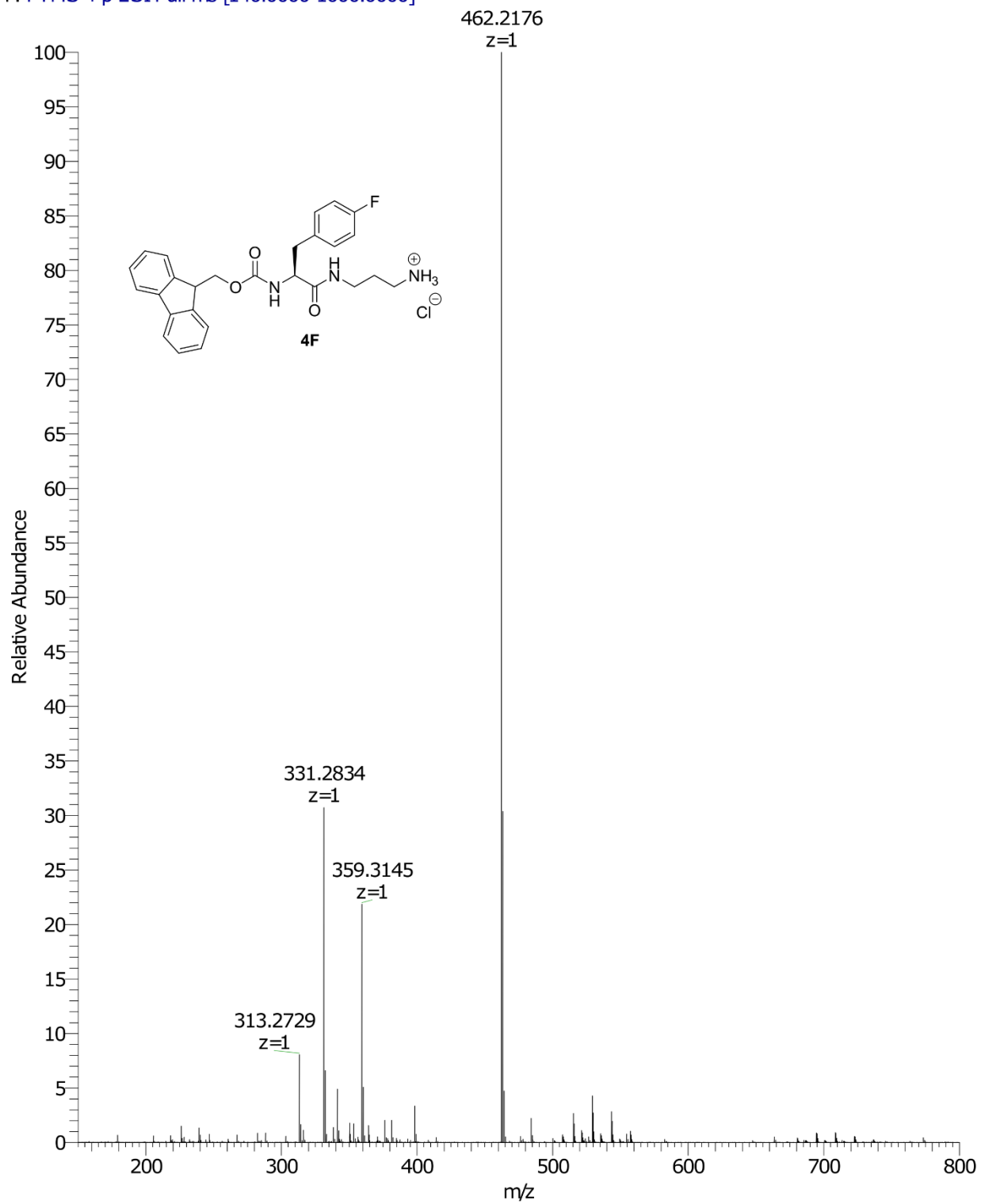


Figure S20. High-resolution mass spectrum of Fmoc-4F-Phe-DAP (4F).

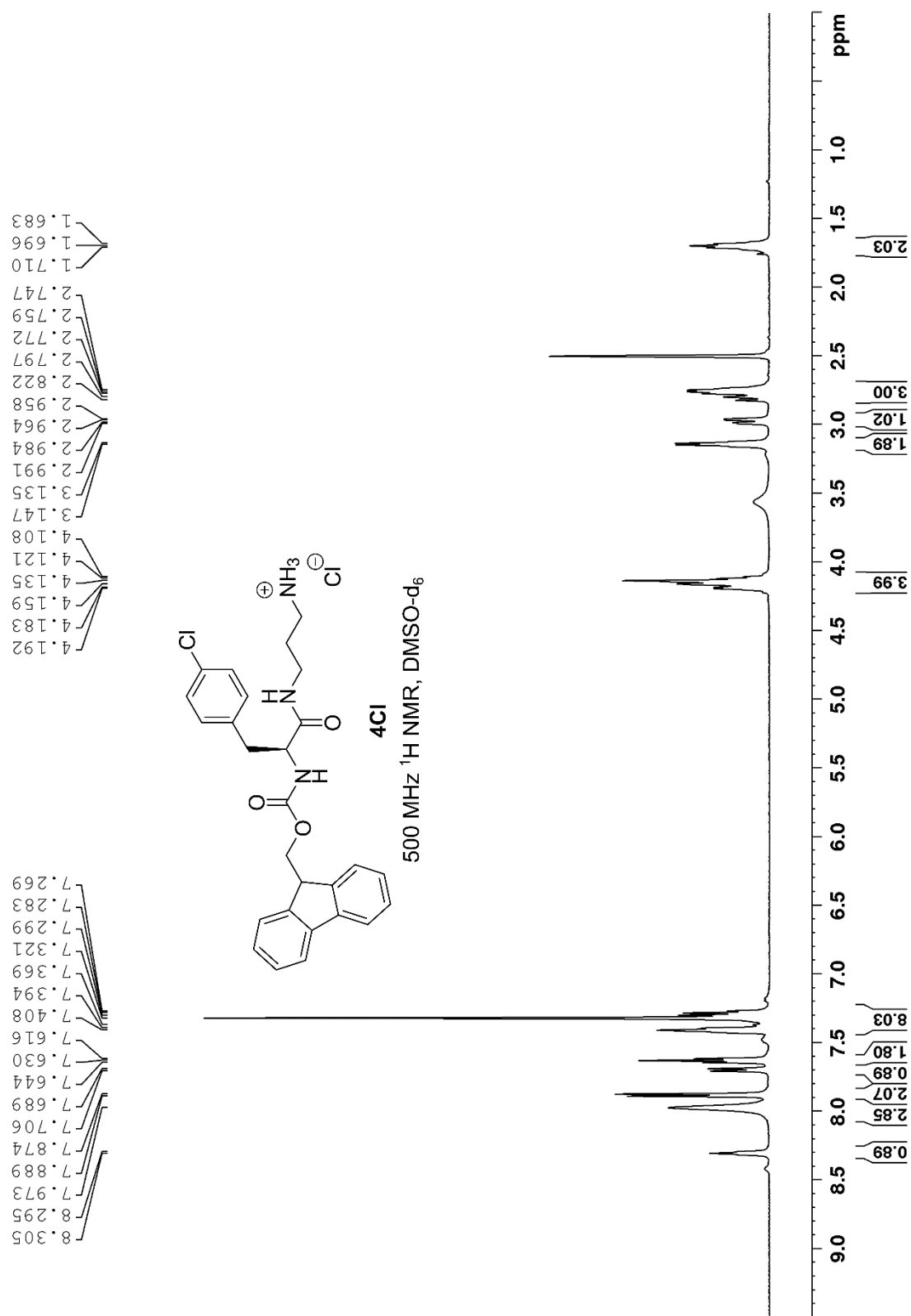


Figure S21. ^1H NMR spectrum of Fmoc-4Cl-Phe-DAP (**4Cl**).

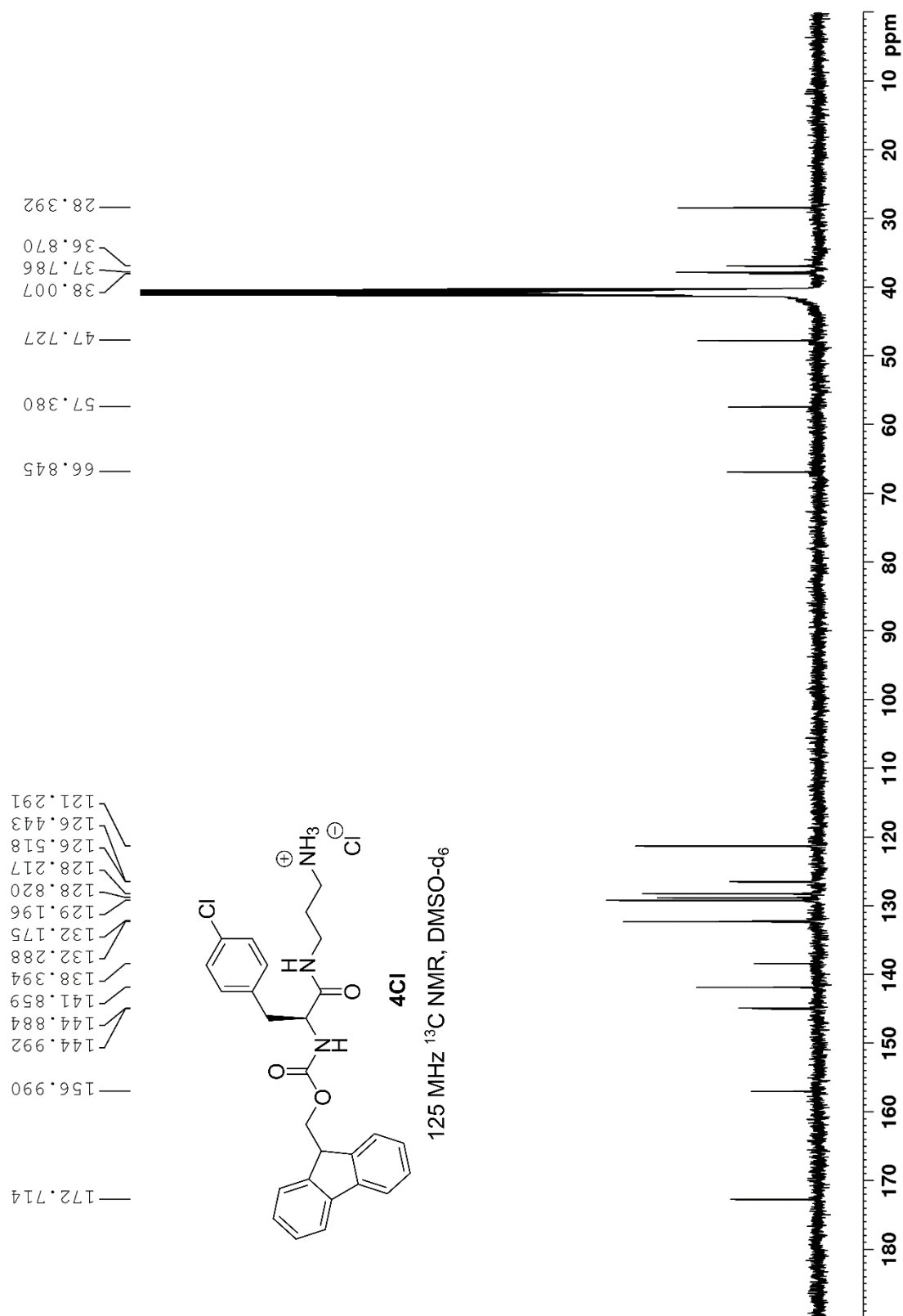


Figure S22. ¹³C NMR spectrum of Fmoc-4Cl-Phe-DAP (**4Cl**).

4Cl #88-181 RT: 0.39-0.80 AV: 94 NL: 9.86E8
T: FTMS +p ESI Full ms [140.0000-1000.0000]

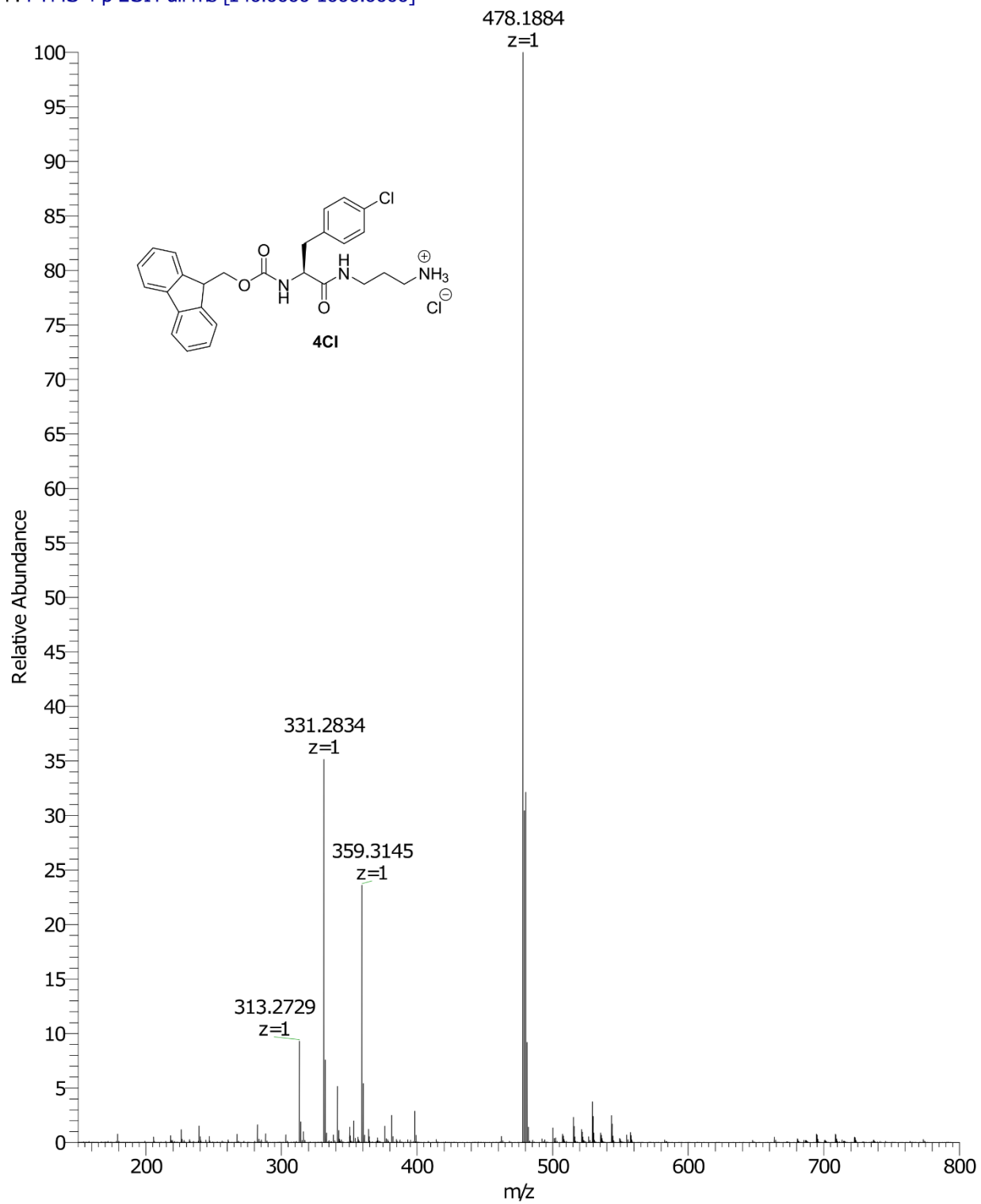


Figure S23. High-resolution spectrum of Fmoc-4Cl-Phe-DAP (4Cl).

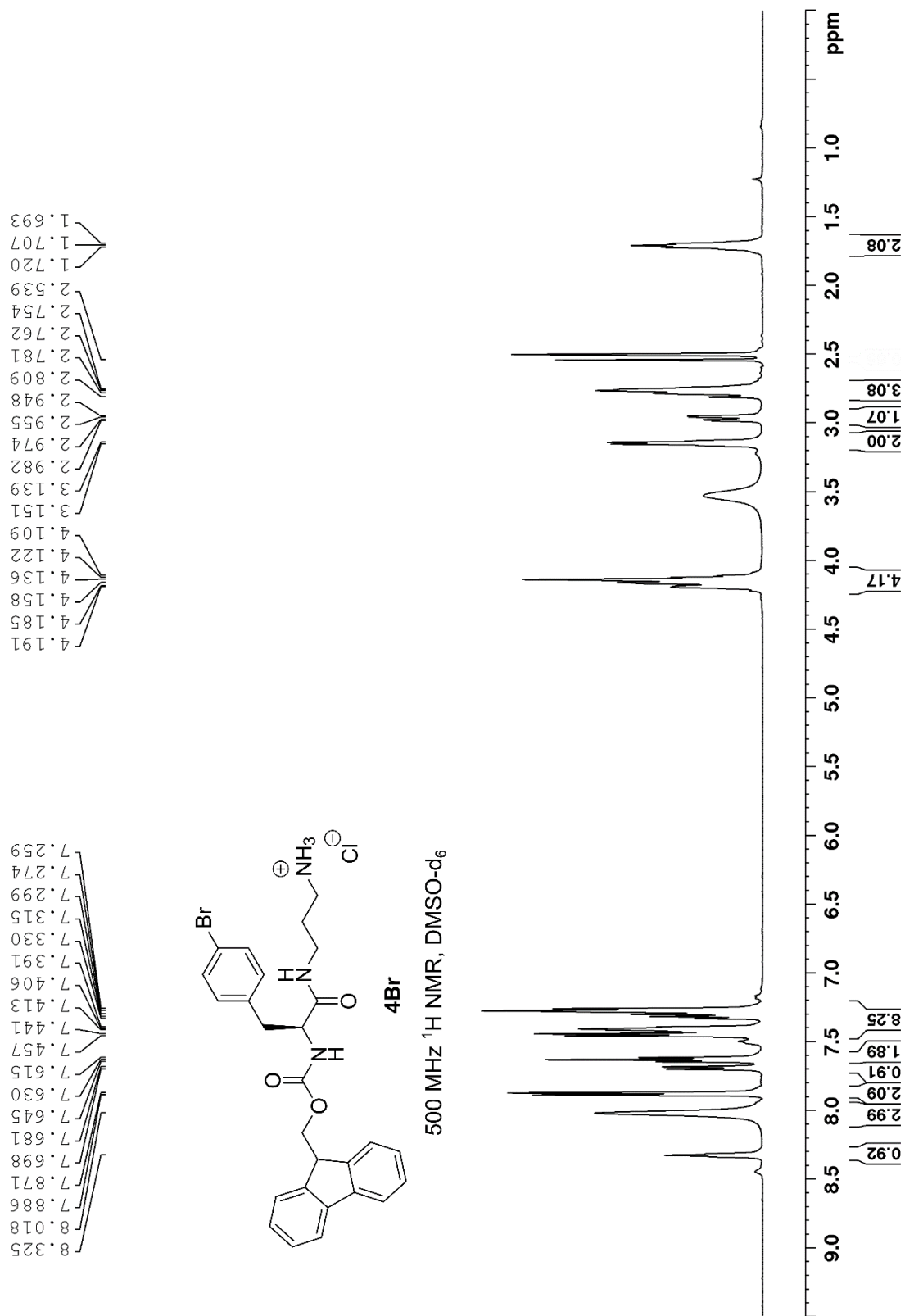


Figure S24. ^1H NMR spectrum of Fmoc-4Br-Phe-DAP (**4Br**).

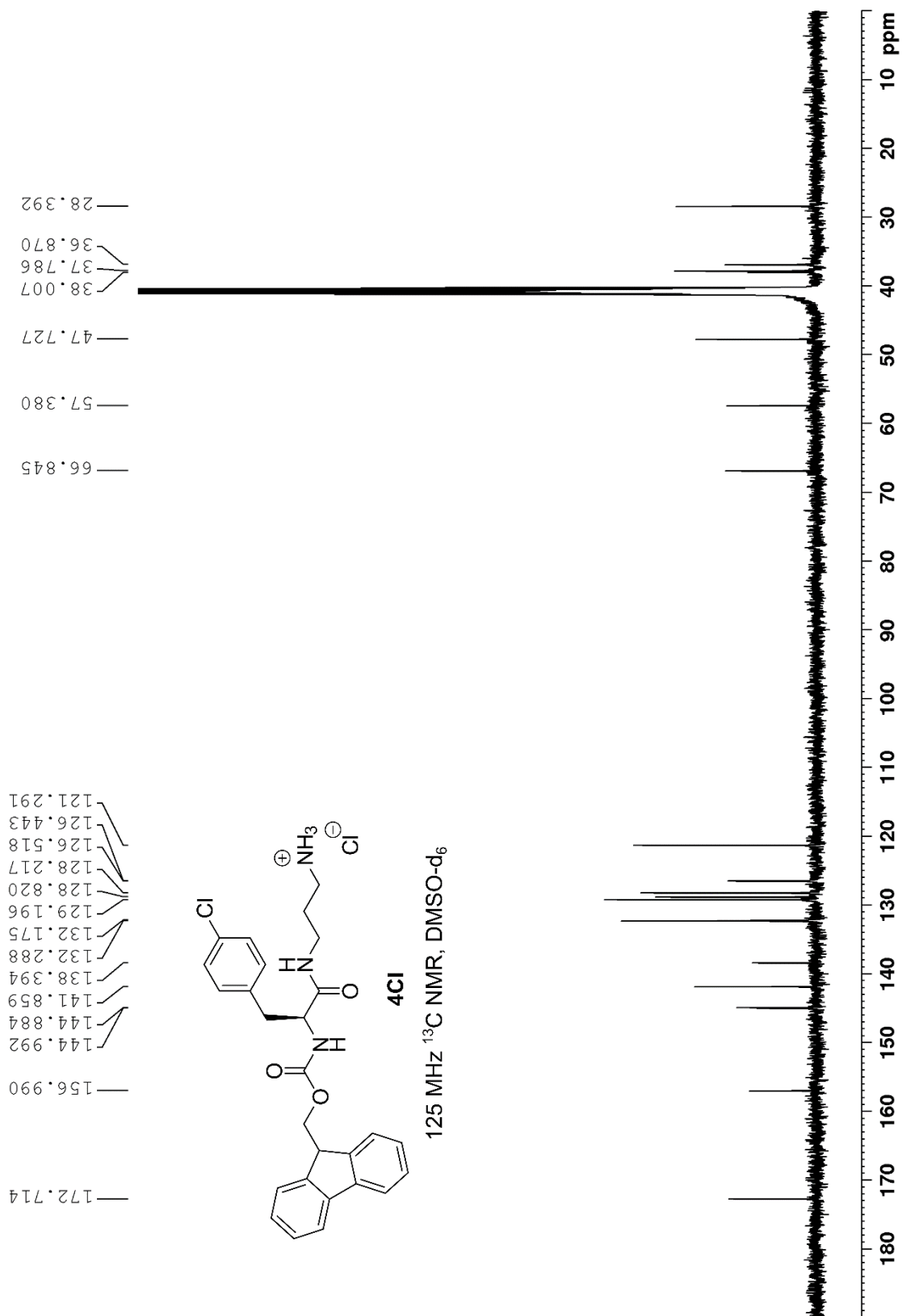


Figure S25. ^{13}C NMR spectrum of Fmoc-4Br-Phe-DAP (**4Br**).

4Br #88-181 RT: 0.39-0.80 AV: 94 NL: 6.67E8
T: FTMS +p ESI Full ms [140.0000-1000.0000]

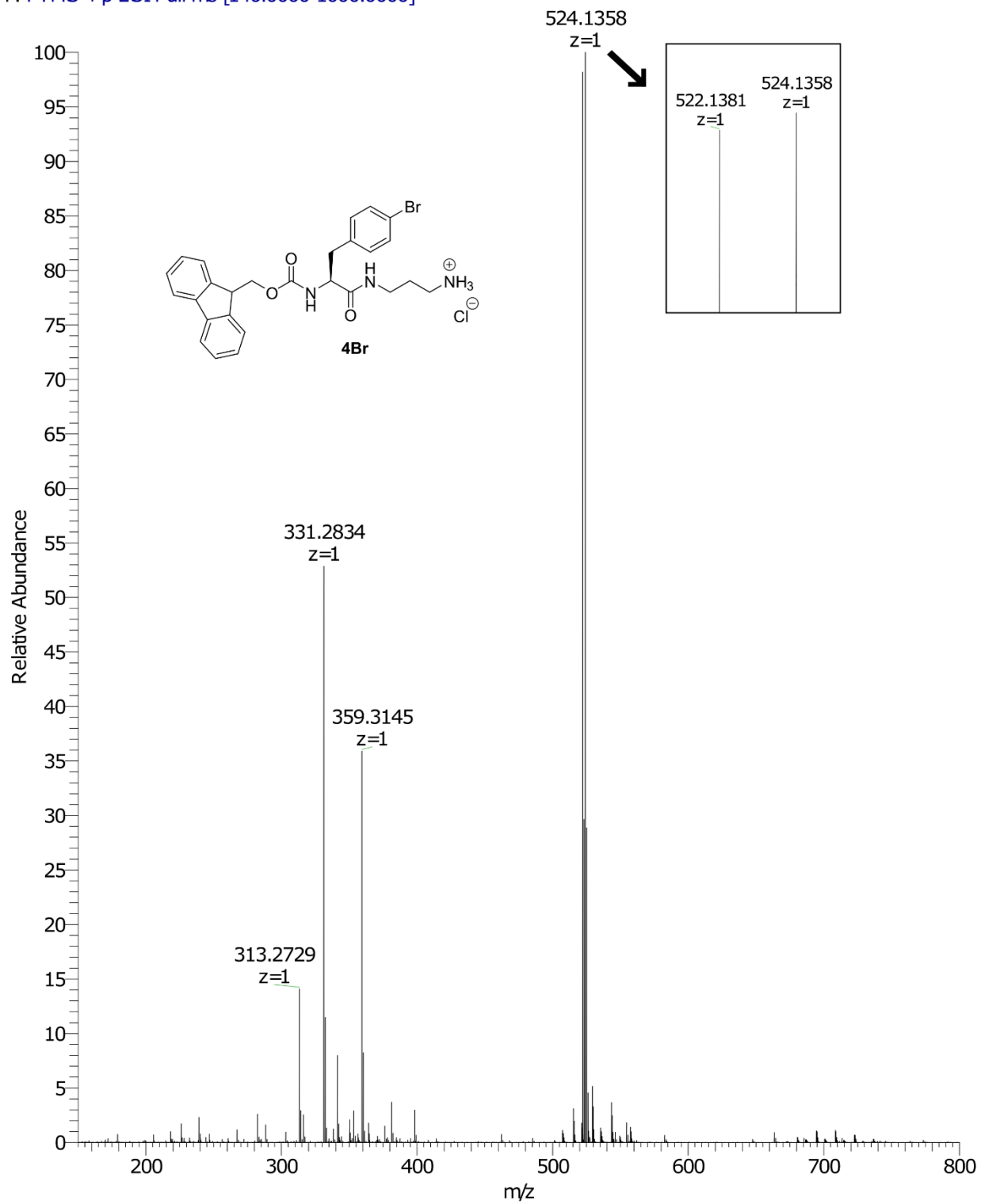


Figure S26. High-resolution mass spectrum of Fmoc-4Br-Phe-DAP (4Br).

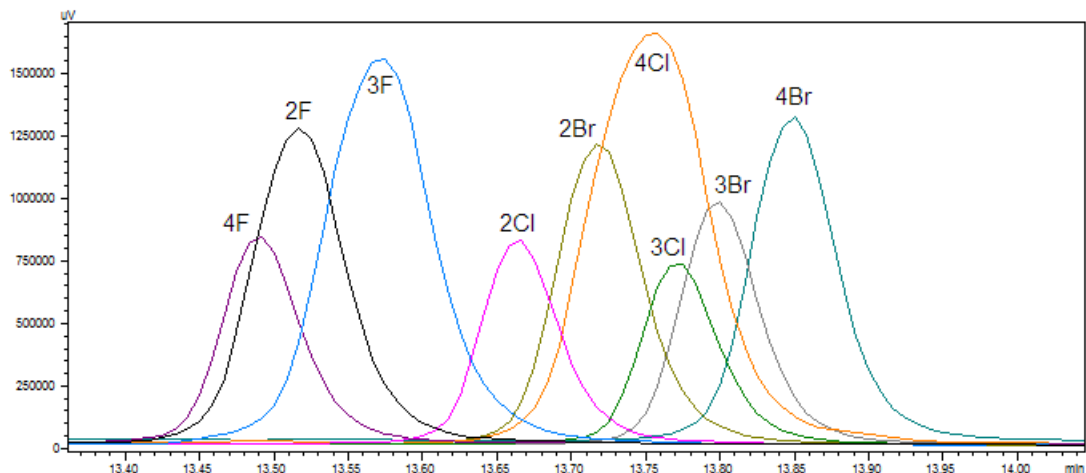


Figure S27. Analytical HPLC traces of compounds **2X–4X** (215 nm).

Table S1. Analytical HPLC method conditions. Each compound was injected onto an analytical HPLC instrument (Shimadzu 2010A) equipped with a Phenomenex Gemini 5 mmC18 column (250 × 4.6mm). A gradient of water (component A) and acetonitrile (component B), both containing 0.05% trifluoroacetic acid, was used as the mobile phase at a flow rate of 1 mL min⁻¹ and UV detection was monitored at 215 nm.

Method Time (min)	%B
0	5
5	5
15	95
20	95
22	5
25	5

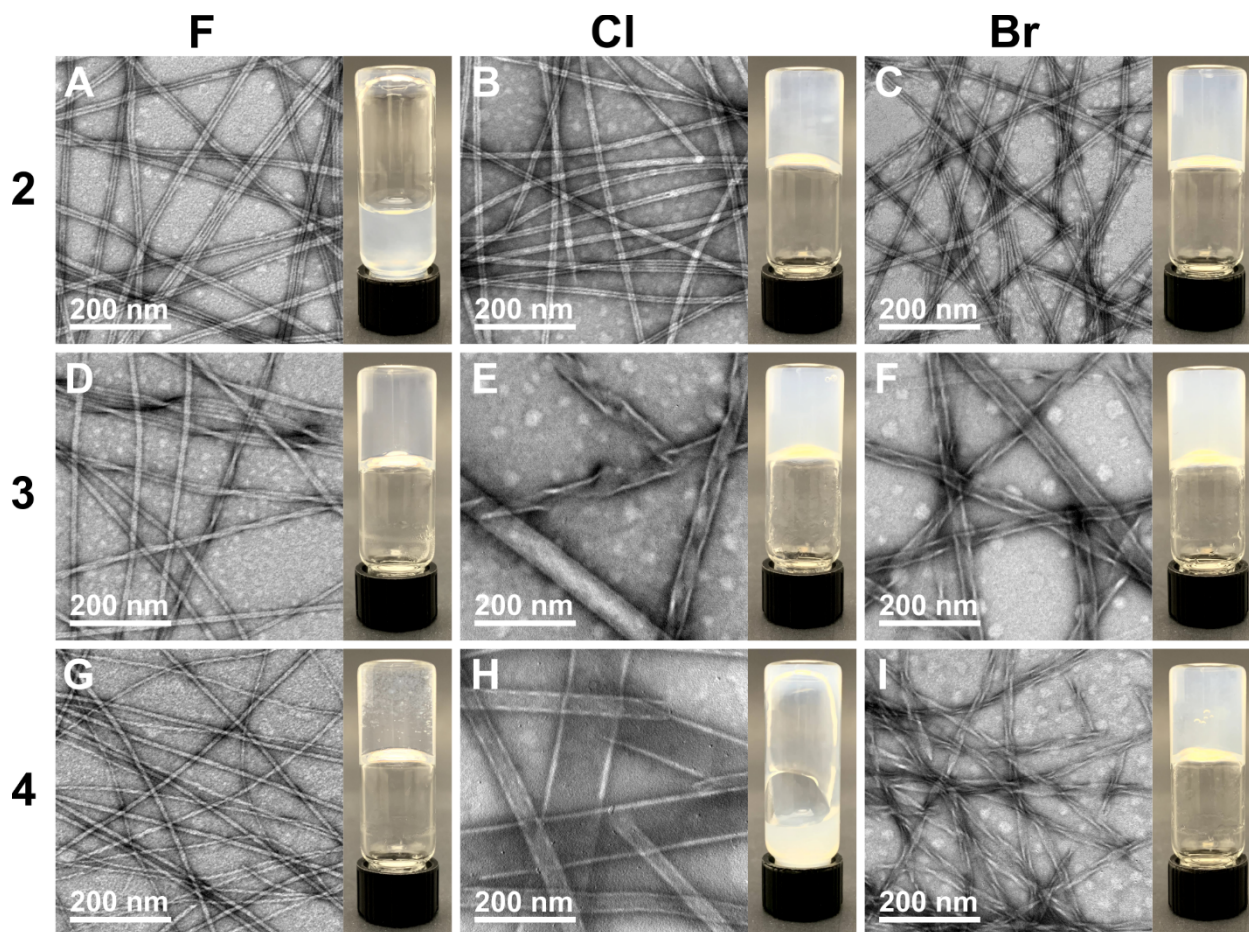


Figure S28. TEM and digital images of assemblies of compounds **2X–4X** taken 1 week after mixing the solution with sodium chloride to initiate self-assembly. (A) Fmoc-2F-Phe-DAP (**2F**); (B) Fmoc-2Cl-Phe-DAP (**2Cl**); (C) Fmoc-2Br-Phe-DAP (**2Br**); (D) Fmoc-3F-Phe-DAP (**3F**); (E) Fmoc-3Cl-Phe-DAP (**3Cl**); (F) Fmoc-3Br-Phe-DAP (**3Br**); (G) Fmoc-4F-Phe-DAP (**4F**); (H) Fmoc-4Cl-Phe-DAP (**4Cl**); (I) Fmoc-4Br-Phe-DAP (**4Br**).

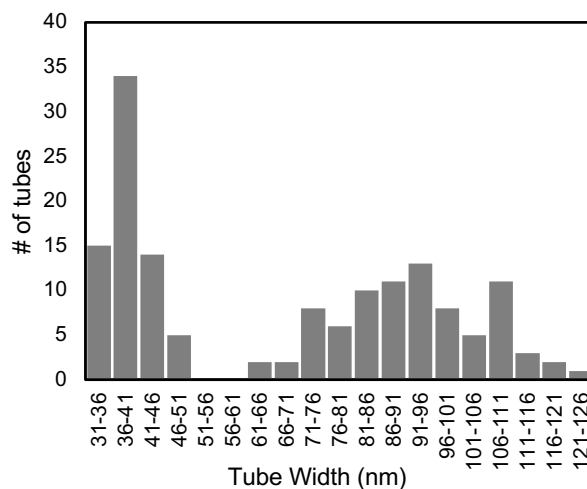


Figure S29. Distribution of nanotube widths in assemblies of Fmoc-4Cl-Phe-DAP (**4Cl**).

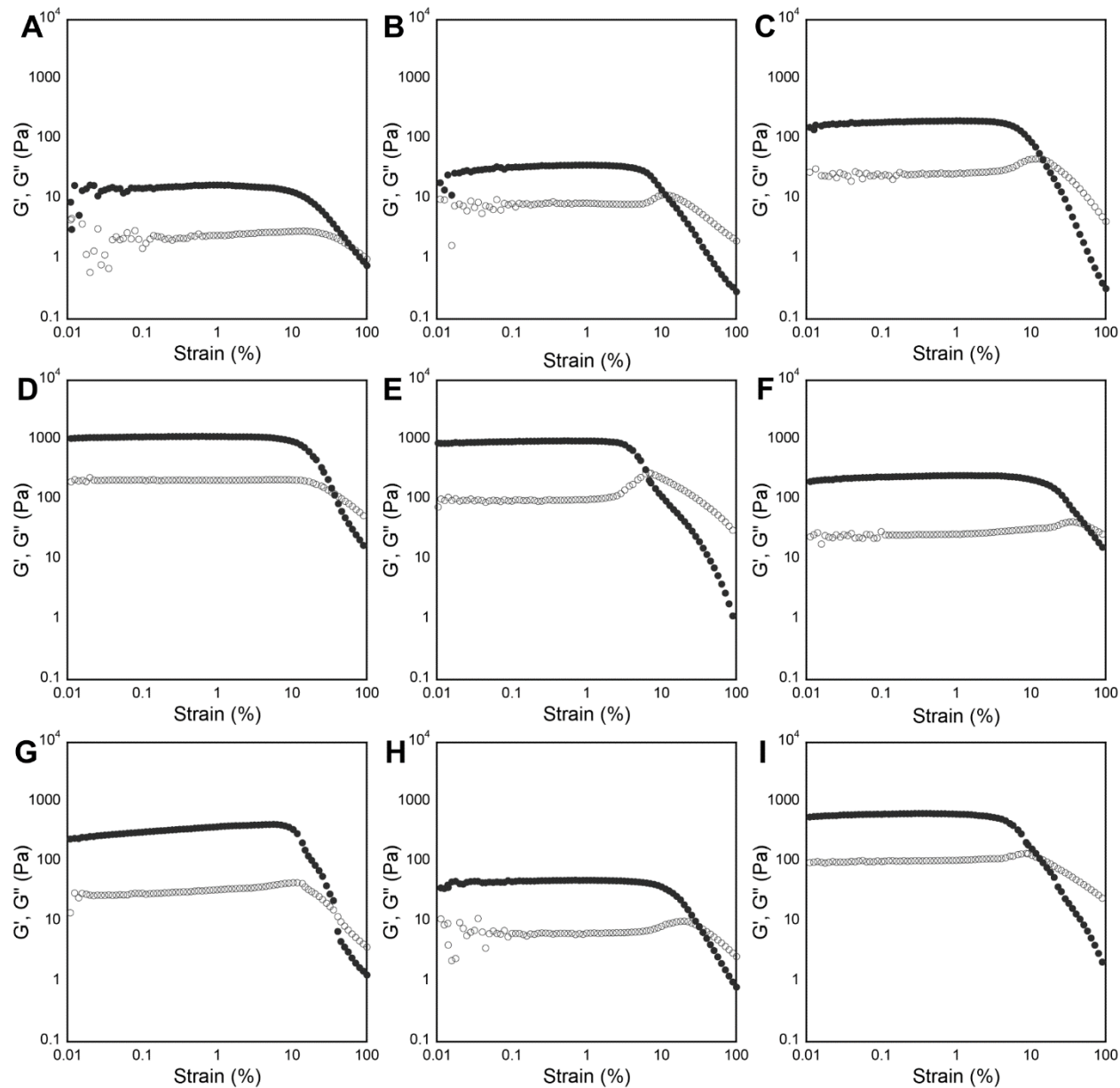


Figure S30. Strain sweep data collected via oscillatory rheology of 10 mM hydrogels of Fmoc-X-Phe-DAP derivatives (**2X–4X**) 24 hours after assembly. G' and G'' values (Pa) are represented by closed circles and open circles, respectively. (A) Fmoc-2F-Phe-DAP (**2F**); (B) Fmoc-2Cl-Phe-DAP (**2Cl**); (C) Fmoc-2Br-Phe-DAP (**2Br**); (D) Fmoc-3F-Phe-DAP (**3F**); (E) Fmoc-3Cl-Phe-DAP (**3Cl**); (F) Fmoc-3Br-Phe-DAP (**3Br**); (G) Fmoc-4F-Phe-DAP (**4F**); (H) Fmoc-4Cl-Phe-DAP (**4Cl**); (I) Fmoc-4Br-Phe-DAP (**4Br**).

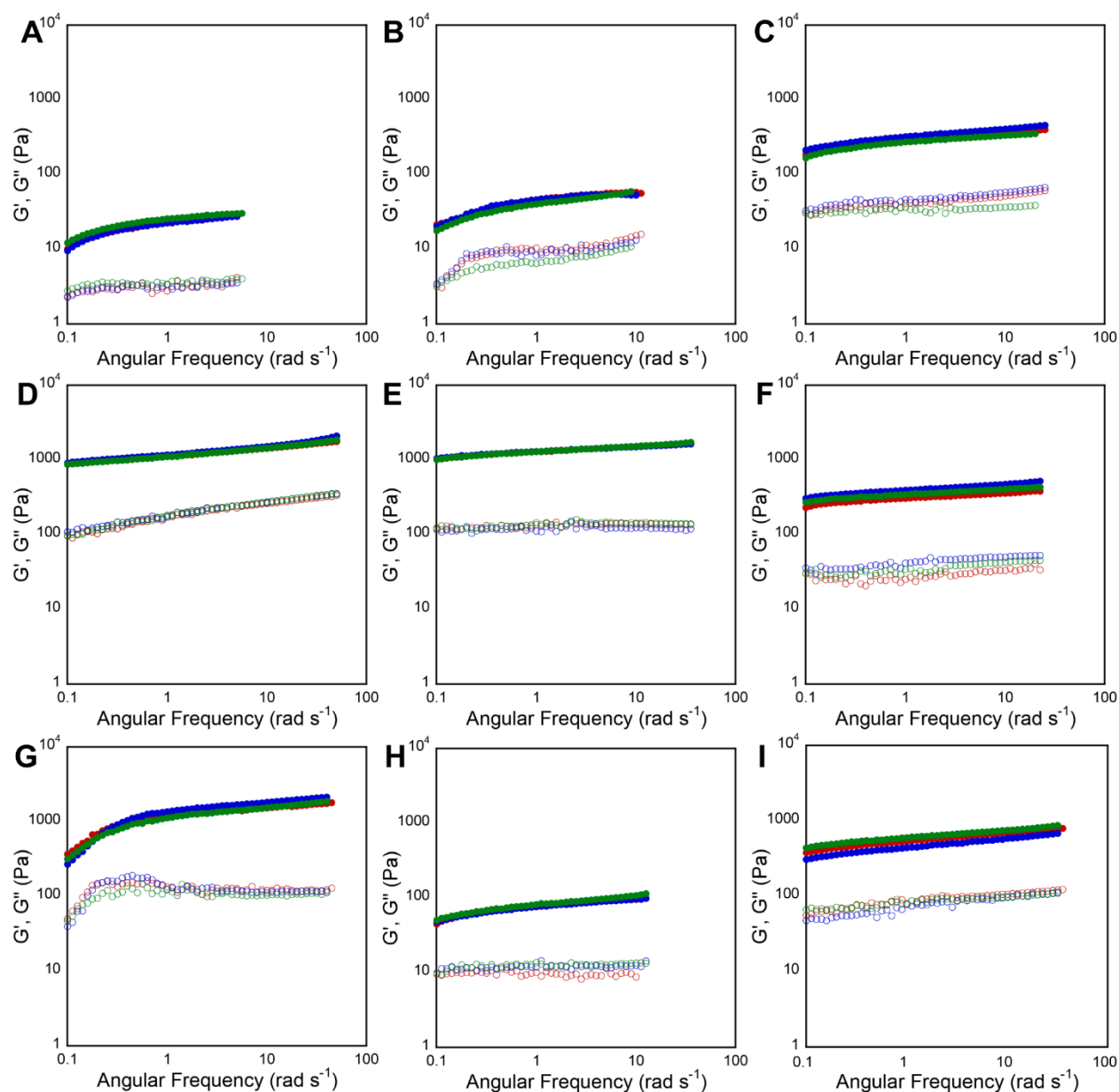


Figure S31. Frequency sweep data collected via oscillatory rheology of 10 mM hydrogels of Fmoc-X-Phe-DAP derivatives (**2X–4X**) 24 hours after assembly. G' and G'' values (Pa) are represented by closed circles and open circles, respectively. Each plot contains three distinct measurements. Values at the upper end of the frequency sweep were cut off when the raw phase angle increased above 175° as recommended for the TA DHR series of rheometers, since values beyond this point are dominated by the instrument inertial torque instead of the sample torque (most prominently seen in samples with low G'/G'' values).³ (A) Fmoc-2F-Phe-DAP (**2F**); (B) Fmoc-2Cl-Phe-DAP (**2Cl**); (C) Fmoc-2Br-Phe-DAP (**2Br**); (D) Fmoc-3F-Phe-DAP (**3F**); (E) Fmoc-3Cl-Phe-DAP (**3Cl**); (F) Fmoc-3Br-Phe-DAP (**3Br**); (G) Fmoc-4F-Phe-DAP (**4F**); (H) Fmoc-4Cl-Phe-DAP (**4Cl**); (I) Fmoc-4Br-Phe-DAP (**4Br**).

References

1. Abraham, B. L.; Toriki, E. S.; Tucker, N. D. J.; Nilsson, B. L. Electrostatic interactions regulate the release of small molecules from supramolecular hydrogels. *J. Mater. Chem. B* **2020**, *8*, 6366-6377.
2. Rajbhandary, A.; Raymond, D. M.; Nilsson, B. L. Self-Assembly, Hydrogelation, and Nanotube Formation by Cation-Modified Phenylalanine Derivatives. *Langmuir* **2017**, *33*, 5803-5813.
3. Ewoldt, R. H.; Johnston, M. T.; Caretta, L. M., Experimental Challenges of Shear Rheology: How to Avoid Bad Data. In *Complex Fluids in Biological Systems: Experiment, Theory, and Computation*, Spagnolie, S. E., Ed. Springer: New York, NY, 2015; pp 207-241.